Rochester Institute of Technology

# RIT Digital Institutional Repository

5-1-1986

# Analysis of compliant pins subjected to plastic deformation

Lincoln Miller

ANALYSIS   OF   COMPLIANT   PINS

SUBJECTED   TO   PLASTIC   DEFORMATION

BY

LINCOLN G. MILLER

IN

PARTIAL   FULFILMENT   FOR   THE   DEGREE   OF

MASTER   OF   SCIENCE

IN

MECHANICAL   ENGINEERING

APPROVED BY:

PROF. _____Hany Ghoneim_____
(Thesis Advisor)

PROF. _____Richard B. Hetnarski_____

PROF. _____Name Illegible_____

PROF. _____B. V. Karlekar_____
(Head of Department)

ROCHESTER   INSTITUTE   OF   TECHNOLOGY

ROCHESTER , N.Y. 14623

MAY , 1986

Title of Thesis   *ANALYSIS OF COMPLIANT PINS*
*SUBJECTED TO PLASTIC DEFORMATION.*

I   Lincoln G. Miller   hereby (grant,
deny) permission to the Wallace Memorial Library, of R.I.T., to
reproduce my thesis in whole or in part.  Any reproduction will
not be for commercial use or profit.

# ACKNOWLEDGEMENTS

# ABSTRACT

An experimental/numerical analysis of two types of compliant pins is presented: dynamic retention pins and cantilever pins. It is shown that there is a trade-off between the performances of both types of pins. For the same range of retention force, the cantilever pin, with a smaller stiffness, is more forgiving and gives a broader range of deflection. The dynamic retention pin is shown to be more reliable with time and replacement frequency, since it exhibits less plastic deformation for the same range of retention force.

# TABLE OF CONTENTS

| | |
|---|---|
| $[K],[K^{\ell}]$ | Stiffness matrix and linear stiffness matrix |
| $\{U\}$ | Nodal value of displacement |
| N,I,1 | Number of elements in finite element structure |
| MSC | MacNeal Schwendler Corporation |
| NASTRAN | NAsa STRuctural ANalysis |
| $\sigma_y$ | Yield stress |
| $\sigma_1$ | Major principal stress |
| $\sigma_2$ | Minor principal stress |
| E | Modulus of elasticity |
| v | Poisson ratio |
| G | Shear modulus of elasticity |
| $\tau$ | Shear stress |
| $\tau_{MAX}$ | Max shear stress |
| $[K^N],[K^M]$ | Stiffness matrix used in Newton and Modified Newton Raphson methods |
| $\{P\},\{P^{\ell}\}$ | Applied load vector |
| $\{\delta\}$ | Vector of unbalanced forces acting at all grid points |
| $\{Q\}$ | Is the unknown vector of constraint forces due to constraints |
| $\{F\}$ | Is the vector of grid point forces due to forces generated by element motion and stress |
| $[K^R]$ | Reference stiffness matrix |
| $\{f^i\}$ | Corrective load vector |
| DOF | Degree of freedom |
| $\epsilon xx, \epsilon yy$ | Directional strain |
| $\tau xx, \tau yy$ | Directional shear stress |

| | |
|---|---|
| $\gamma_{xy}$ | Directional shear strain |
| $\sigma_{xx}, \sigma_{yy}$ | Directional stresses |
| $\epsilon_{ij}$ | Tensor notation for strain |
| $U_i, U_j$ | Tensor notation for displacement |
| PSI | Pounds per square inch |
| Mils | $10^{-3}$ Inch |
| $\psi$ | Shape function |
| $\Gamma$ | Boundary |
| $\Omega$ | Domain |
| I | Moment of inertia |
| PC | Printed circuit |
| k | Hardening parameter |
| $W_p$ | Plastic work |
| $d\bar{\epsilon}_p$ | Effective plastic strain |
| $(d\epsilon_{ij})p$ | Plastic component of strain |
| $H'$ | Strain hardening parameter |
| $\bar{\sigma}$ | Effective stress |
| $d\epsilon_p$ | Plastic strain increment |
| $\underset{\sim}{a}$ | Flow vector |
| $d\lambda$ | Plastic multiplier |
| [D] | Matrix of elastic constants |
| [Dep] | Elasto-plastic matrix |
| $\rho$ | Density |
| $\underset{\sim}{b}$ | Body force vector |
| [B] | Strain/Displacement matrix |

INTRODUCTION


## 1.1 PRESS-FIT PINS (COMPLIANT PINS)


The interconnection of electrical components has been
achieved by various techniques over the last twenty years.
Initially, soldering was the most widely used method for
reliability and longevity of the connection.  With the arrival
of solderless wrap technology [1,3], and the significant
economic advantages it brought about, without compromise
to reliability and longevity of the connection, pressure
connections have been gaining wider acceptance in printed
circuit (PC) boards.

The Press-Fit pin connection technology is based on
the principle of providing a pressure connection, so that there
is adequate and continous metal-to-metal contact during
the expected life of the two connecting components.  The elastic
energy that is necessary to maintain the pressure connection is
stored in one or both of the components [1,2,3].

Easier manufacturing, assembly, repair and replacements
make pressure connection technology very effective.  Also, the
absence of related soldering problems such as contamination,
solder splashes and localized heating  [1,3],  favors the
economic and practical acceptance of the Press-Fit pin
technology.

A good Press-Fit pin has to satisfy several design objectives [1]:

. The pin could be used over a wider range of hole sizes in the PC board.

. The pin had to store most of its elastic energy.

. Less damage to the expensive PC board during insertion of the pins.

. Less plastic deformation for the same level of retention force.

. Reliability of connection and inexpensive replacement.

A compliant pin with a wide range of elasticity and moderate stiffness would satisfy the above objectives.


1.2 SCOPE OF STUDY


This study is devoted to analyzing the performance of two types of compliant pins: the dynamic retention pin, which is presently in use; and the cantilever pin, which is proposed herein (Figures 1 and 2). The analysis is carried out using a numerical technique, the finite element method (MSC/NASTRAN) as well as experimental testing.

Most engineering designs are based exclusively on the theory of elasticity, although it is widely recognized that the yield stress is often exceeded. In this study, both pins are compared within the same range of retention force for a wide range of deflection.
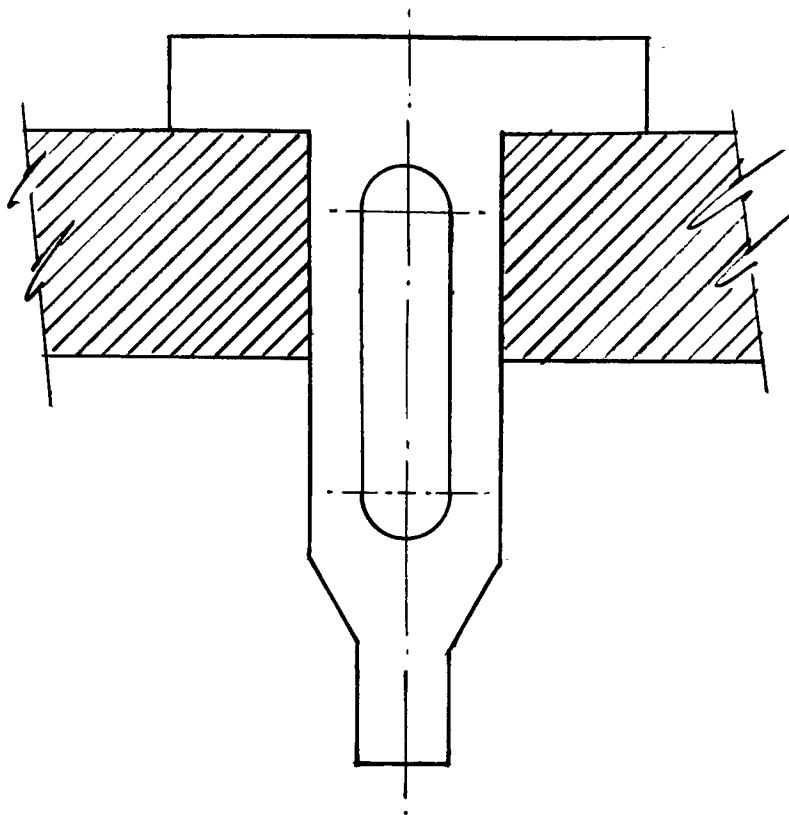
Figure 1    Schematic of the Dynamic Retention Pin
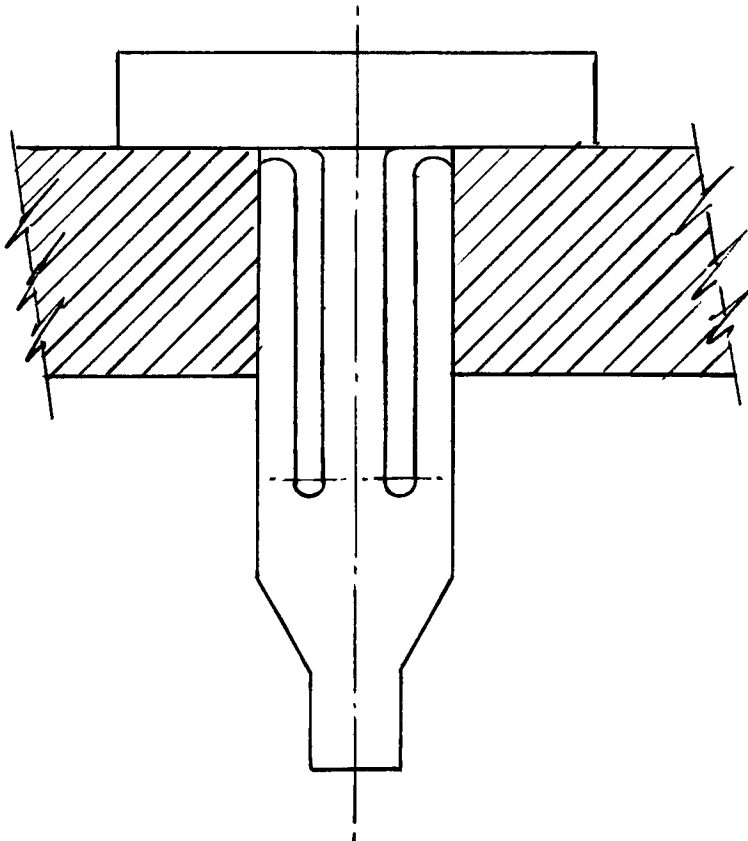


Figure 2    Schematic of the Cantilever Pin

In the numerical models, sections within the printed circuit boards are loaded uniformly and other sections are assumed to have small gaps. Symmetrical boundary conditions are applied to other appropriate sections of the models.

Experimental work is conducted using an Instron TTD machine. A qualitative analysis of the flexibility of both types of pins is performed from their load-deflection diagrams.

## 2. FINITE ELEMENT ANALYSIS

## 2.1    MSC/NASTRAN

NASTRAN was formulated and developed under the sponsorship of the National Aeronautics And Space Administration (NASA) based on requirements of the aerospace industry for structural analysis. MSC (MacNeal Schwendler Corporation) markets its own version, MSC/NASTRAN, that has the capability of solving a wide range of engineering problems.

MSC/NASTRAN non-linear analysis, SOL 66, with plastic deformation option is the numerical tool of this study.

## 2.2    FINITE  ELEMENT  THEORY

### 2.2.1  NON-LINEAR  ANALYSIS

Non-linearities occur in two different forms in finite element analysis. The first is geometric non-linearity, which results from finite changes in the geometry of the deforming body. The second is material or physical non-linerity, which results from the non-linear constitutive laws [4,5]. Material non-linearity is easier to

visualize. It entails problems in which stresses are non-linearly proportional to the strains, but in which only small displacements and small strains are considered.

For the solution of Mechanics problems, the basic finite element equation is utilized (see Equation (n), Appendix 2).

$$[K] \{U\} = \{F\} \tag{1}$$

Where [K] is the structual stiffness matrix

   {U} is the nodal displacement vector

   {F} is the applied nodal forces

For non-linear problem, such as plasticity, the non-linearity occurs in the stiffness matrix [K] (see Equation (v),Appendix 3). In general, when the coefficients of the matrix [K] depend on the unknown displacememts {U}, or their derivatives, the problem becomes non-linear [6].

The solution of Equation (1) is tedious to solve directly. As a result, an iterative approach has to be taken.


## 2.2.2 ITERATIVE TECHNIQUES AND STIFFNESS MATRIX UPDATE

The Newton-Raphson and Modified Newton-Raphson iteration techniques are used to solve the non-linear equation systems.

A single degree-of-freedom non-linear force function, F(u), (Figures 3 and 4) can be written as:

$$F(u)^{N+1} = F(u)^{N} + (u^{N+1} - u^{N}) \frac{\partial F(u)}{\partial U}$$

(by using Taylor's series expansion neglecting higher order terms)

Stiffness concept can be defined as :

$$K(u) = \frac{\partial F(u)}{\partial U}$$

The Newton-Raphson iteration recurrsion equation can be written as :

$$[K^{N}]\{U^{N+1} - U^{N}\} = \{P\} - \{F^{N}\} \tag{2}$$

Where at a given iteration n

$[K^{N}]$ is the current value of the stiffness matrix

$\{U^{N+1}\}$ is the new value of the displacement vector

$\{U^{N}\}$ is the current value of the displacement vector

$\{P\}$ is the vector for applied external loads

$\{F^{N}\}$ is the current value of the grid point force vector

$\{F^{N}\}$ has to be computed accurately as a function of $\{U^{N}\}$ and $[K^{N}]$ may be approximated, but convergence will be dependent on the choice of $[K^{N}]$.

In the Modified Newton-Raphson iteration recurrsion equation:

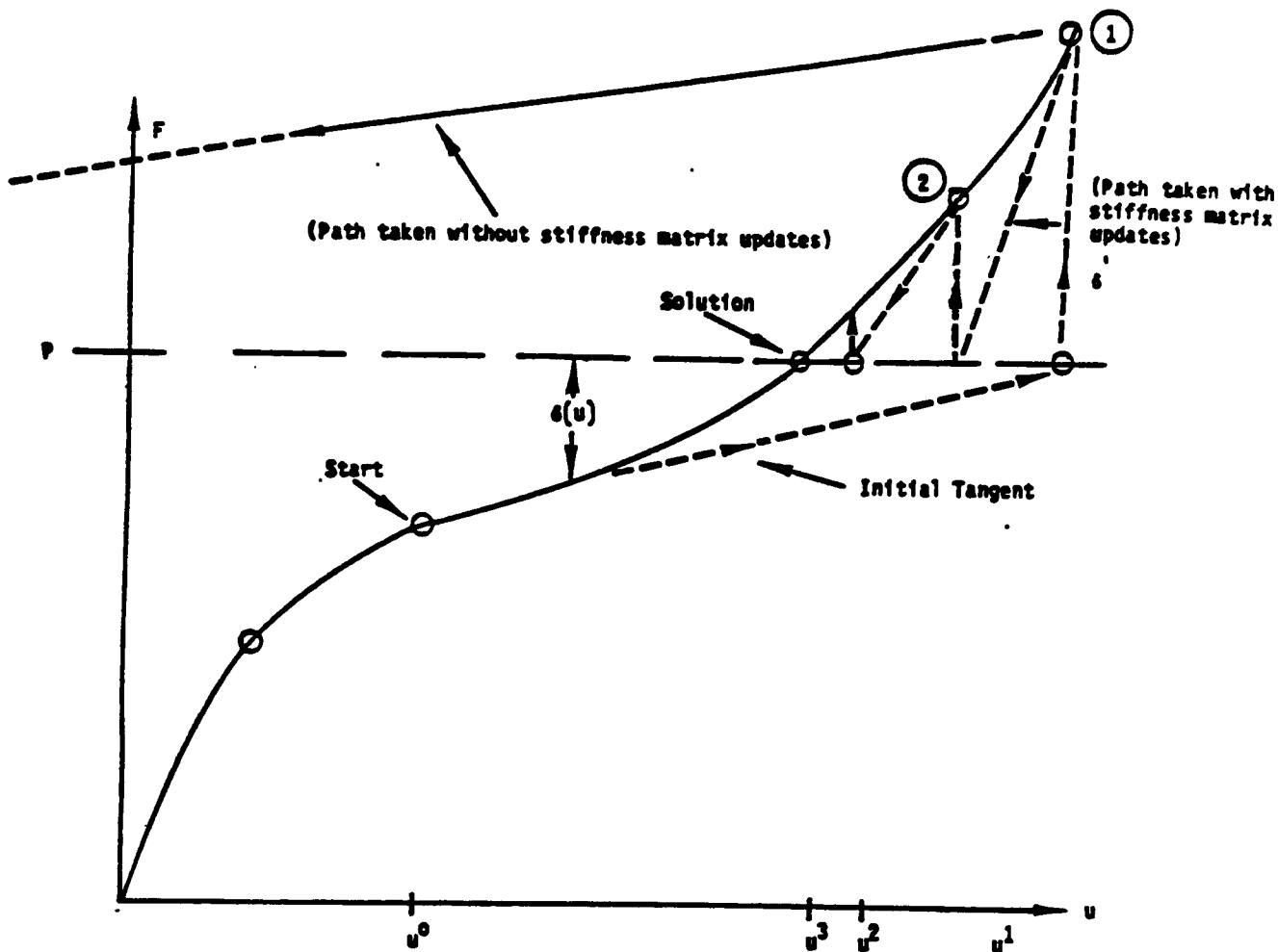$$[K^{M}]\{U^{N+1} - U^{N}\} = \{P^{L}\} - \{F^{N}\} \tag{3}$$

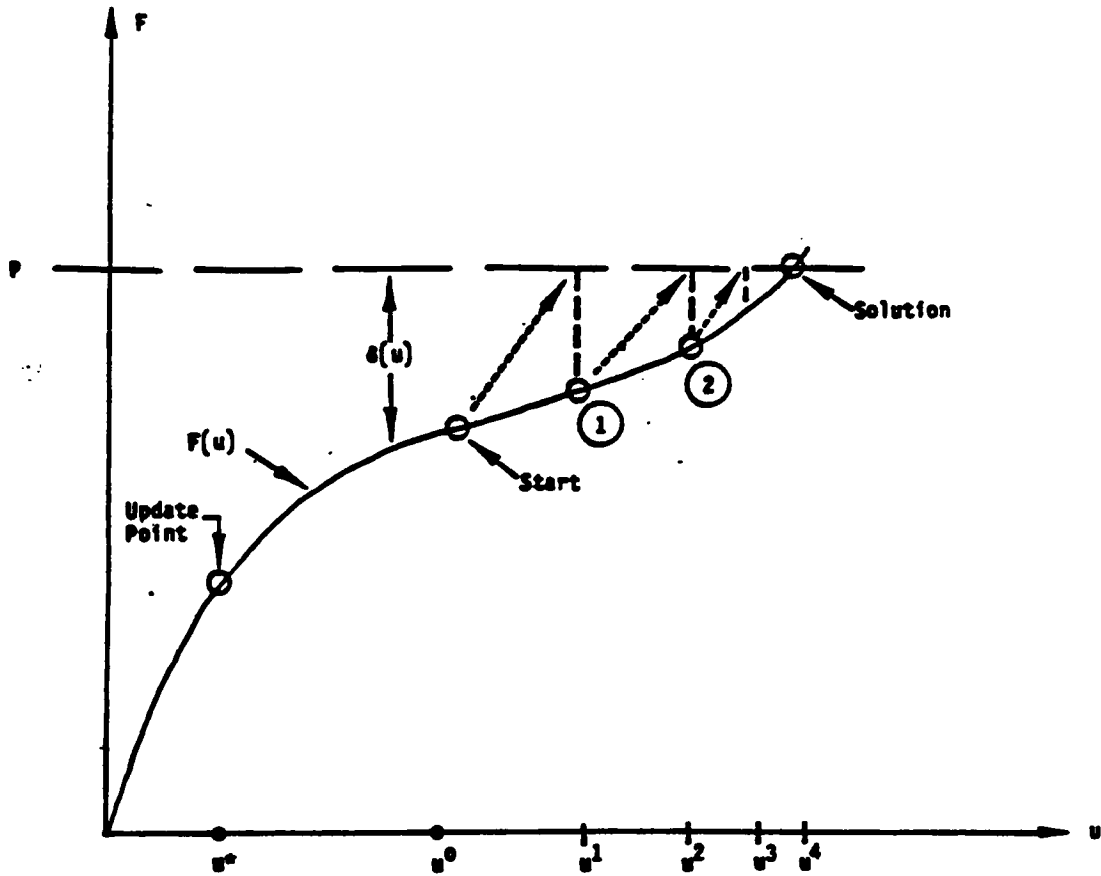Figure 3 Single DOF Iteration - Updates of Stiffness Matrix.

Figure 4 Single DOF Iteration - No Stiffness Matrix Updates.

Where: $\{F^{N}\}$     changed at each iteration

       $[K^{M}]$     changed less frequently or not at all

       $\{P^{L}\}$     changed less frequently or not at all


Figures 3 and 4 show the procedures of both methods, Newton-Raphson and Modified Newton-Raphson respectively, employed by MSC/NASTRAN for non-linear iteration. The curves show a single DOF non-linear force function. The dashed lines show the iteration paths, with slopes equal to the reference matrix $[K^{R}]$. The method of Figure 3 is to be used in this study.

In MSC/NASTRAN the method used to obtain a solution is by minimizing the error vector $\{\delta\}$ given by [8] :

$$\{\delta\} = \{P\} + \{Q\} - \{F\} \tag{4}$$

where    $\{\delta\}$ is the error vector of unbalanced forces acting at grid point components.

     $\{P\}$ is the vector of applied external loads, which may change with displacements.

     $\{Q\}$ is the unknown vector of constraint forces.

     $\{F\}$ is the vector of grid point forces generated by element motion and stress. The terms are functions of displacement, temperature and stress history.

It should be noted that degrees of freedom not involved in constraints produce null terms in $\{Q\}$ and that dependent

constraint points produce no errors. Therefore, when Equation
(4) is reduced to the solution coordinates the constraint forces
{Q} disappear. Terms in the vector {F} are dependent on the
deformations of the finite elements. In linear static analysis
the vector {F} becomes :

$$\{F_{LINEAR}\} = [K^{\ell}] \{U\} - P^{T}(T) \tag{5}$$

where $P^{T}$ is the "Thermal load vector"

For non-linear solution a "Reference" matrix $[K^{R}]$ (slopes
of Figures 3 and 4, that change stiffness matrix update) is
used, in which the terms are derivatives in the form [8] :

$$[K^{R}] = \left. \frac{\partial F_i}{\partial U_j} \right|_{U = U^{R}} \tag{6}$$

If $\{U^{R}\}$ is a known displacement with error $\{\delta(U^{i})\}$, then
Newton's method may be used to predict a new vector $\{U^{i+1}\}$
with smaller error. Using Taylor's Series expansion and
negelecting higher order terms the non-linear force is
approximately:

$$\{F(U)\} \cong \{F(U^{i})\} + [K^{R}]\{U - U^{i}\} \tag{7}$$

Substituting Equation (7) into Equation (4) with $\{\delta\} = 0$

$$[K^{R}]\{U - U^{i}\} \cong \{P\} + \{Q\} - \{F(U^{i})\} \tag{8}$$

Which can be written in terms of the error vector $\{\delta\}$ to
provide the format of the Newton-Raphson iteration method:

$$[K^R] \{ U^{i+1} - U^i \} = \{ \delta ( U^i ) \} \tag{9}$$

When $[K^R]$ is inverted , Equation (9) may be used to solve for $\{ U^{i+1} \} = \{ U \}$, a new estimate of the solution.

Equation (9) provides an incremental form for solution iteration.   Another form of the iteration equation is obtained from Equations (4) and (9):

$$[K] \{ U^{i+1} - U^i \} = \{ P \} + \{ Q \} + \{ P^T \} - \{ f^i \} \tag{10}$$

Where :
$$\{ f^i \} = \{ F ( U^i ) \} - [K^R] \{ U^i \} + \{ P^T \} \tag{11}$$

$\{ f^i \}$   equal zero when $\{ F \}$ is linear and $[K^R]$ contains
    linear elastic terms.

Equation (9) is quite useful since load error $\{ \delta \}$ and incremental displacements $(U^{i+1} - U^i)$ are available for testing convergence [8].

Equations (9), (10) and (11) are used in MSC/NASTRAN for non-linear iteration.

## 2.2.3   YIELD  CRITERION

For a material in simple tension, there exist a yield point at which the material will begin to deform plastically. For a general state of stress, a yield criterion is required to define which combination of stresses will cause yielding [6,11].

The Von-Mises yield criterion, also known as the Hencky-Mises yield criterion, states that yielding begins when the distortion energy exceeds a critical value [6,8,11]. In simple tension, this critical value is equal to the yield stress [$\sigma y$], that is :

$$\frac{1}{2} \{ [\sigma_1 - \sigma_2]^2 + [\sigma_2 - \sigma_3]^2 + [\sigma_3 - \sigma_1]^2 \} = \sigma y^2 \tag{12}$$

For the case of pure shear in two dimensions :
$$\sigma_1 = -\sigma_2 = \tau \quad ; \quad \sigma_3 = 0$$

Equation (12) becomes :

$$\tau = \frac{\sigma y}{\sqrt{3}} \tag{13}$$

Equation (13) states that the yield stress in pure shear is $1/\sqrt{3}$ times the yield stress in tension.

Another yield criterion, referred to as the Maximum Shear Theory or Tresca yield criterion states that when the maximum shear stress reaches the value of the maximum shear stress occuring under simple tension, yielding will occur [6,8,11].

For the case of pure shear :

$$\sigma_1 = -\sigma_2 = \tau_{MAX} , \qquad \sigma_3 = 0$$

The maximum shear stress theory predicts yielding to occur when :

$$\sigma_1 - \sigma_2 = 2\tau_{MAX} = \sigma y$$

$$\text{or } \tau_{MAX} = \frac{1}{2} \sigma y \tag{14}$$

That is, the yield stress in pure shear is one-half (1/2) the yield stress in simple tension.

The Von-Mises yield criterion predicts a pure shear yield stress which is about fifteen percent higher than that predicted by the Tresca criterion.

The Von-Mises yield criterion usually fits the experimental data better than the other theories, and it is generally easier to apply than the Tresca criterion, because the relative magnitudes of the principal stresses need not be known [11]. For these reasons, the Von-Mises yield criterion is used in this study.

## 2.2.4   HARDENING   EFFECT

When a plastically deformed specimen is unloaded, residual stresses on a microscopic scale remain and influence the plastic yielding if the specimen undergoes additional loads. If the previous strain was a uniform extension and the specimen is then reloaded in compression in the opposite direction, it is observed that yielding occurs at a much reduced stress [6,7,8],

giving rise to hardening effects, the Bauschinger effect.

The Bauschinger effect is represented in Figure 5. It is assumed that the elastic unloading range is twice the initial yield stress. If the initial yield stress in tension is $\sigma y$ and the specimen is loaded up to stress $\sigma_1$ and unloaded, the new plastic yielding in compression at $\sigma_2$, given by :

$$\sigma_2 = \sigma_1 - 2\sigma y$$

This is shown by path OABCD, which states that the total elastic range of the material remains constant since the initial compressive yield is reduced by the same amount as the tensile yield is raised. This strain hardening model is said to be kinematic (Figure 5).

The path OABGH shows that the hardening mechanism is acting equally in tension and compresion, that is $\sigma_2 = -\sigma_1$ (Figure 5). This is referred to as isotropic hardening.

When it is assumed that the tensile and compressive yields are independent of each other, then the compressive yield is at $-\sigma y$, which is not dependent on the amount of tensile hardening (path OABEF). This phenomenom is referred to as combined isotropic and kinematic hardening.

These three hardening options can be programmed into MSC/NASTRAN for the models. Isotropic hardening option is used in this study.
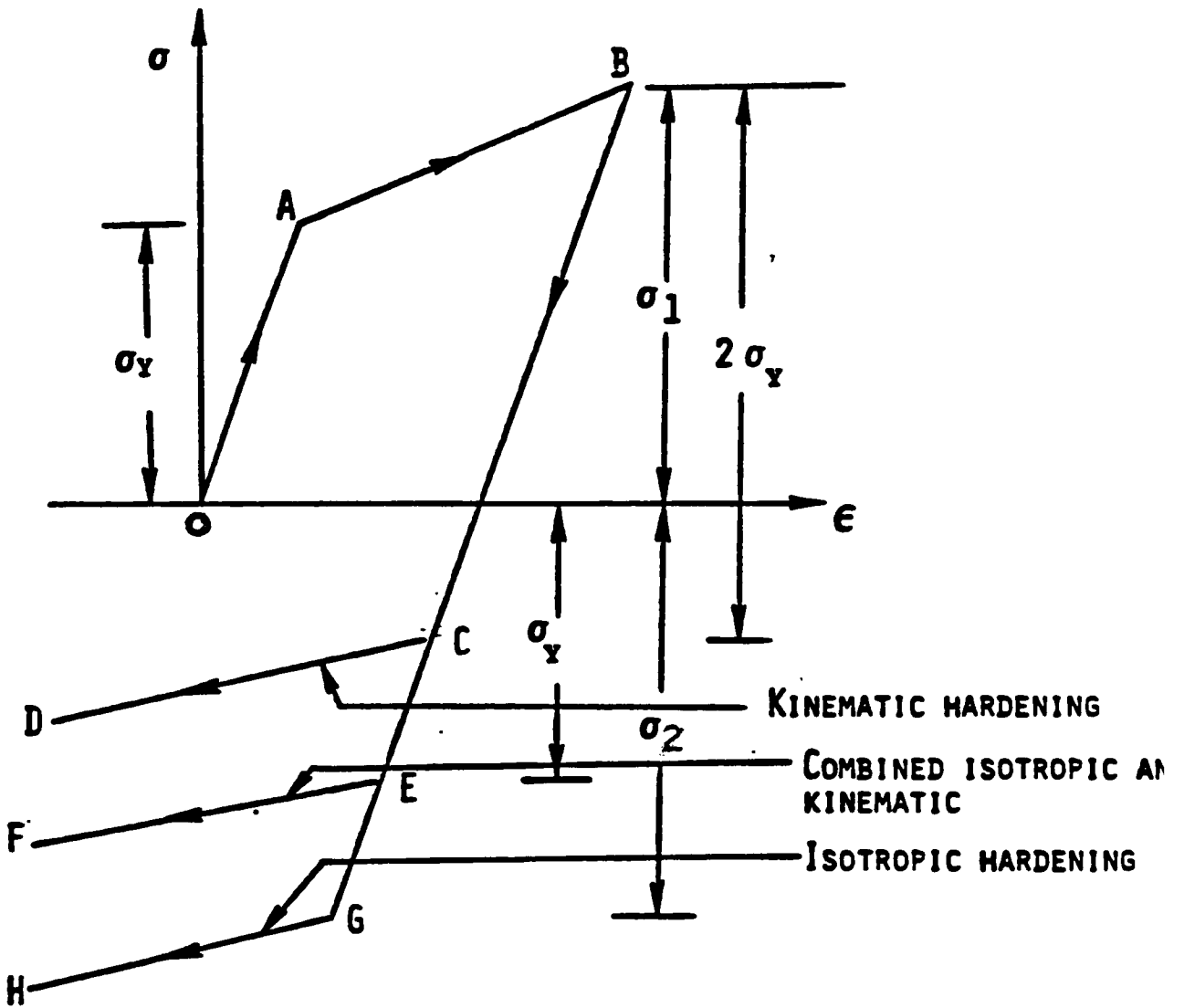
Figure 5     REPRESENTATION OF BAUSCHINGER EFFECT

## 2.3   FINITE ELEMENT MODEL

The finite element method is used as the basic numerical technique to study the elastic-plastic deformation of the two compliant pins (Figures 1 and 2).

The compliant pins have symmetrical characteristics, and these are used to reduce modelling effort and subsequent computer run time.  In general, when a structure has symmetrical boundary conditions and loading, the resultant stress field will also be symmetrical.  As a result, no additional information is gained by reproducing identical stress fields across planes of symmetry [10].

Model data such as coordinates, element definition, element "connectivity", and material properties  are generated and programmed into the computer for finite element analysis.  The pins are modelled using MSC/NASTRAN QUAD4 and TRIA3 elements [see Programs].

In this study GAP elements, specified on CGAP and PGAP Bulk Data cards, are used to model surfaces of the complaint pins and PC boards which may come into contact.  A GAP element connects two grid points which initially is coincident [8].  Within the PC boards (60 +/- 3 Mils thick) GAP elements are used for 30-40 Mils sections for the  dynamic retention  and cantilever pins respectively.

Loading of sections of the cantilever and dynamic retention
pins within the PC boards (20-30 Mils) are achieved by using
enforced displacements (SPCD in Bulk Data [16]) of 0.65, 1.5 and
3 Mils for the three SUBCASES.  The loading sequence is
controlled by LOAD request in the Case Control Data.  Also,
FORCE Bulk Data cards with directions of loading are used.

Boundary conditions are applied to the symmetrical and load
sections of the compliant pins (SPC1 Bulk Data cards [16]).
Along these sections the displacements are constrained ($Ux = 0$).
The point O shown on Figures 6(a) and 7(a) for the element
layouts are constrained both for $Ux=0$ and $Uy=0$ in order to fix
that point.

NLPARM cards [15] used in Case Control and Bulk Data
selects and defines a set of parameters for non-linear analysis
iteration strategy.  Each SUBCASE (in Case Control) defines a
new total load and iteration method defined by the NLPARM Bulk
Data.  The change in loads between the three SUBCASES is further
subdivided into evenly spaced increments by the LINC field on
the requested NLPARM card.  AUTO and AUTOQN are the iteration
methods used for modelling.  The AUTO method provides automatic
matrix update and the AUTOQN method provides additional accuracy
over the AUTO method (additional internal searching and less
chance of a diverging solution).  The number of iterations per
load increment are controlled by using the MAXITER option in the
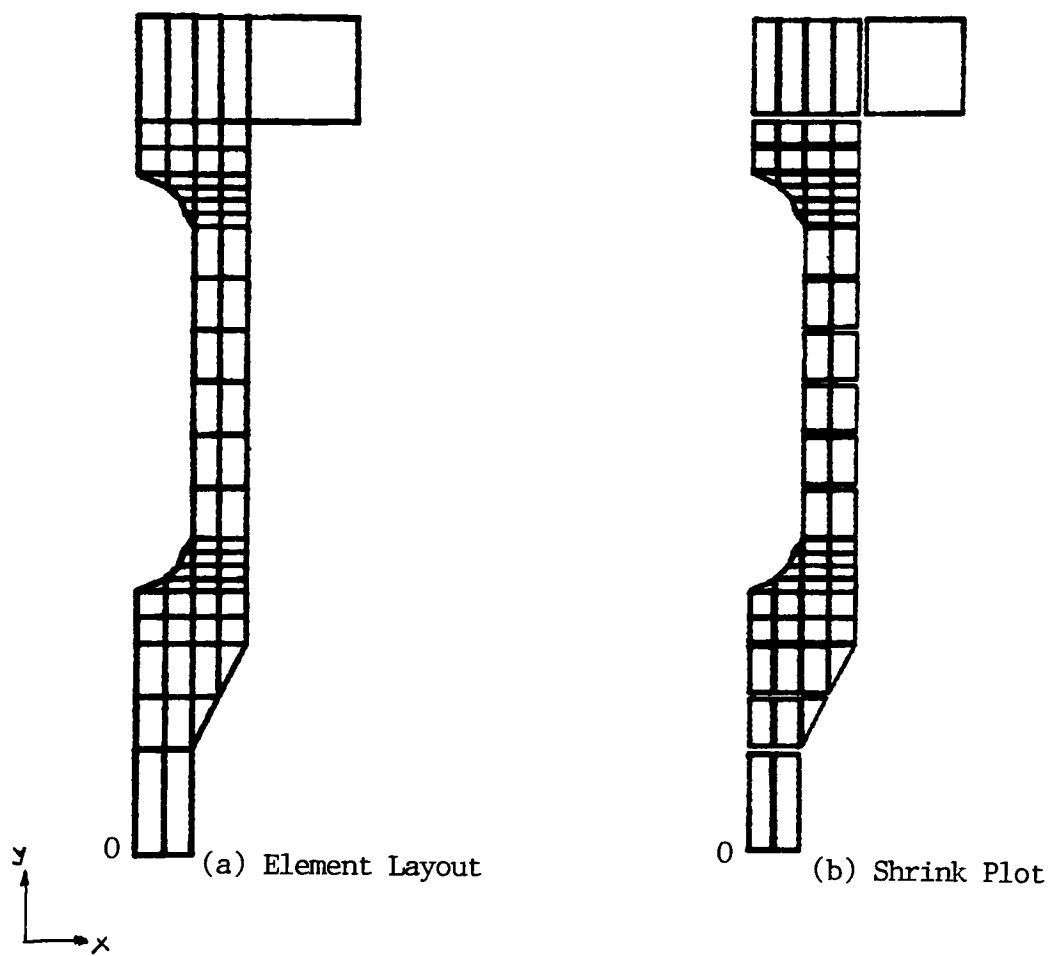NLPARM Bulk Data.  Also, the number of diverging solutions

(a) Element Layout    (b) Shrink Plot

Figure 6    Finite Element Layout of the Dynamic Retention Pin
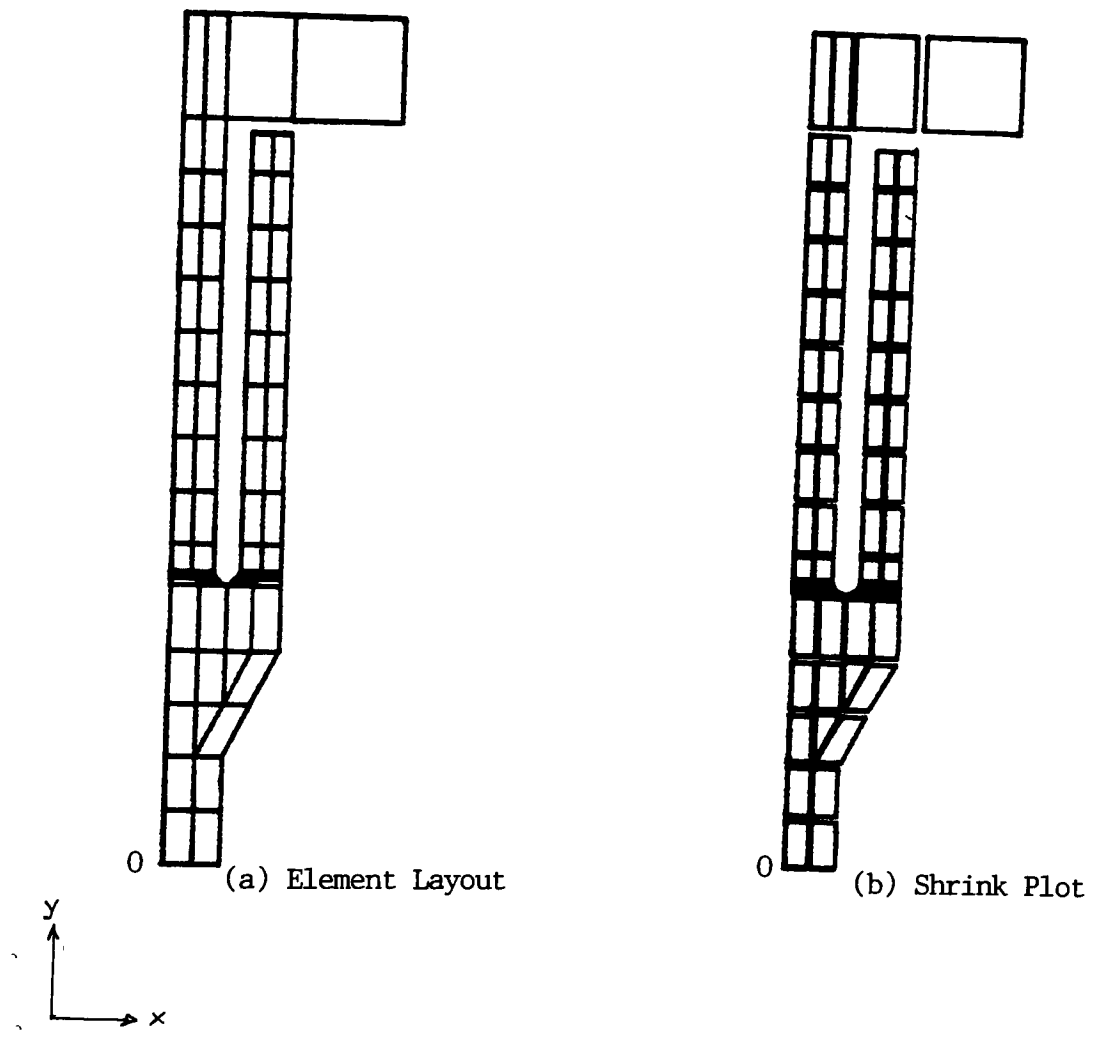
(a) Element Layout          (b) Shrink Plot

Figure 7   Finite Element Layout of the Cantilever Pin

allowed before the non-linear iterations stop are controlled by the MAXDIV option in the NLPARM Bulk Data.

The selection of the type of non-linearity and the non-linear characteristics of the material of the compliant pins are modelled using the MATS1 Bulk Data card [15]. PLASTIC (Elastoplastic) option is used as the type of material non-linearity. Other options that are used include work hardening slope (slope of stress vs. plastic strain) of zero for elastic-perfectly plastic case, isotropic hardening effect and the Von-Mises yield criterion. Also used is the factor for yield stress, $\sigma_y$. On a stress-strain relation the slope of the line joining the origin to the yield stress is equal to the value of the Modulus of Elasticity, E.

Figures 6(a & b) and 7(a & b) show the finite element layouts and shrink plots of the dynamic retention and cantilever pins. Since the pins are retangular in cross section, plane stress conditions are assumed for the models. Also, damage due to insertion of pins in PC boards, sliding and frictional effects are neglected.

# 3. EXPERIMENTAL TESTING

Large scale models (25 X )of the two types of compliant
pins (Figures 8 and 9) were tested in compression using an
Instron TTD machine.  Figure 10 shows a schematic of an Instron
machine and model set up.

During experimental testing, loadings are to be applied
in approximately the same area as the numerical models.  Also,
loadings are to be applied at reasonable speeds (0.05 - 0.1
inch/min).

The Load-Deflection diagram is to be used to provide
information on the flexibility of both pins, so that qualitative
analysis can be made and compared with results obtained from the
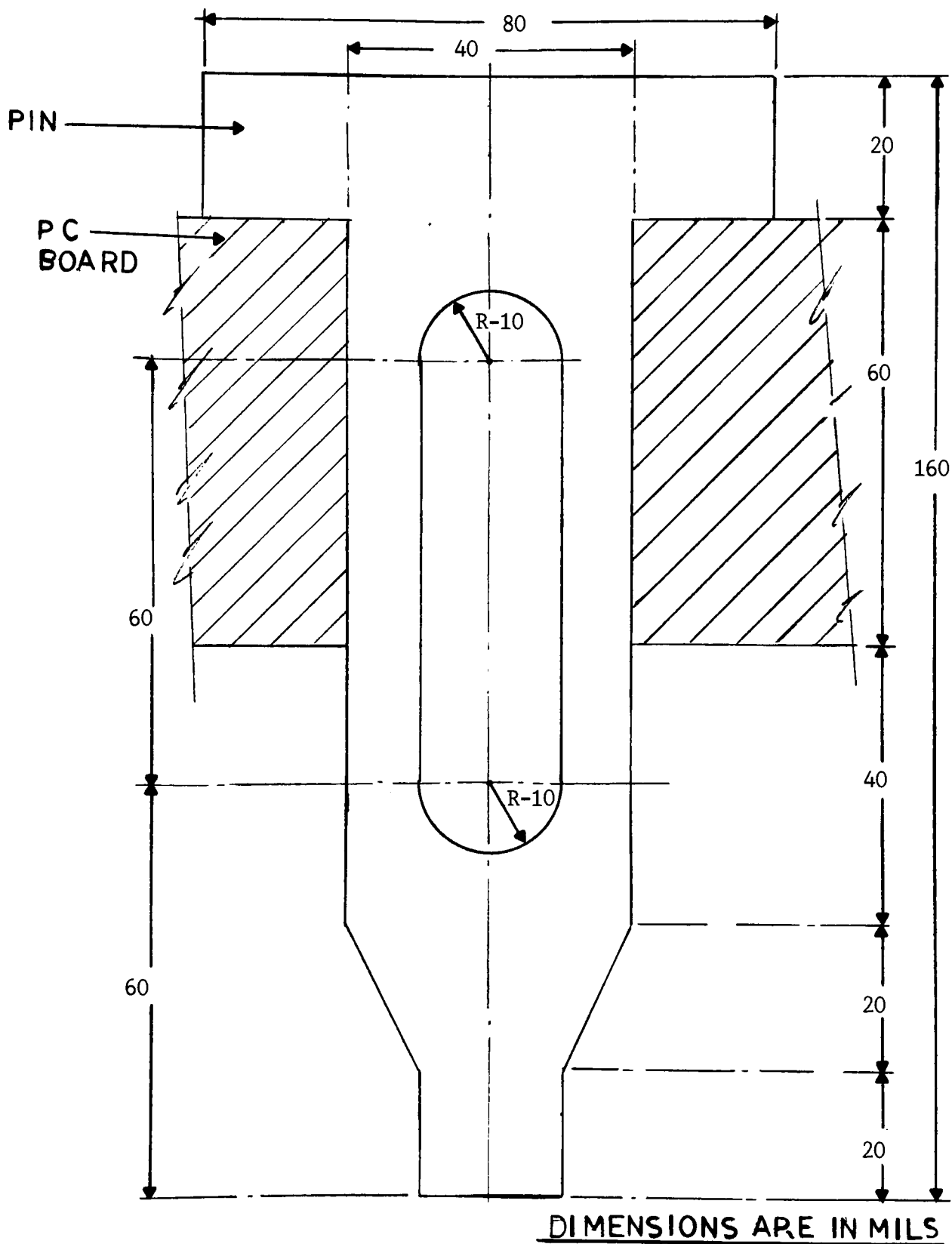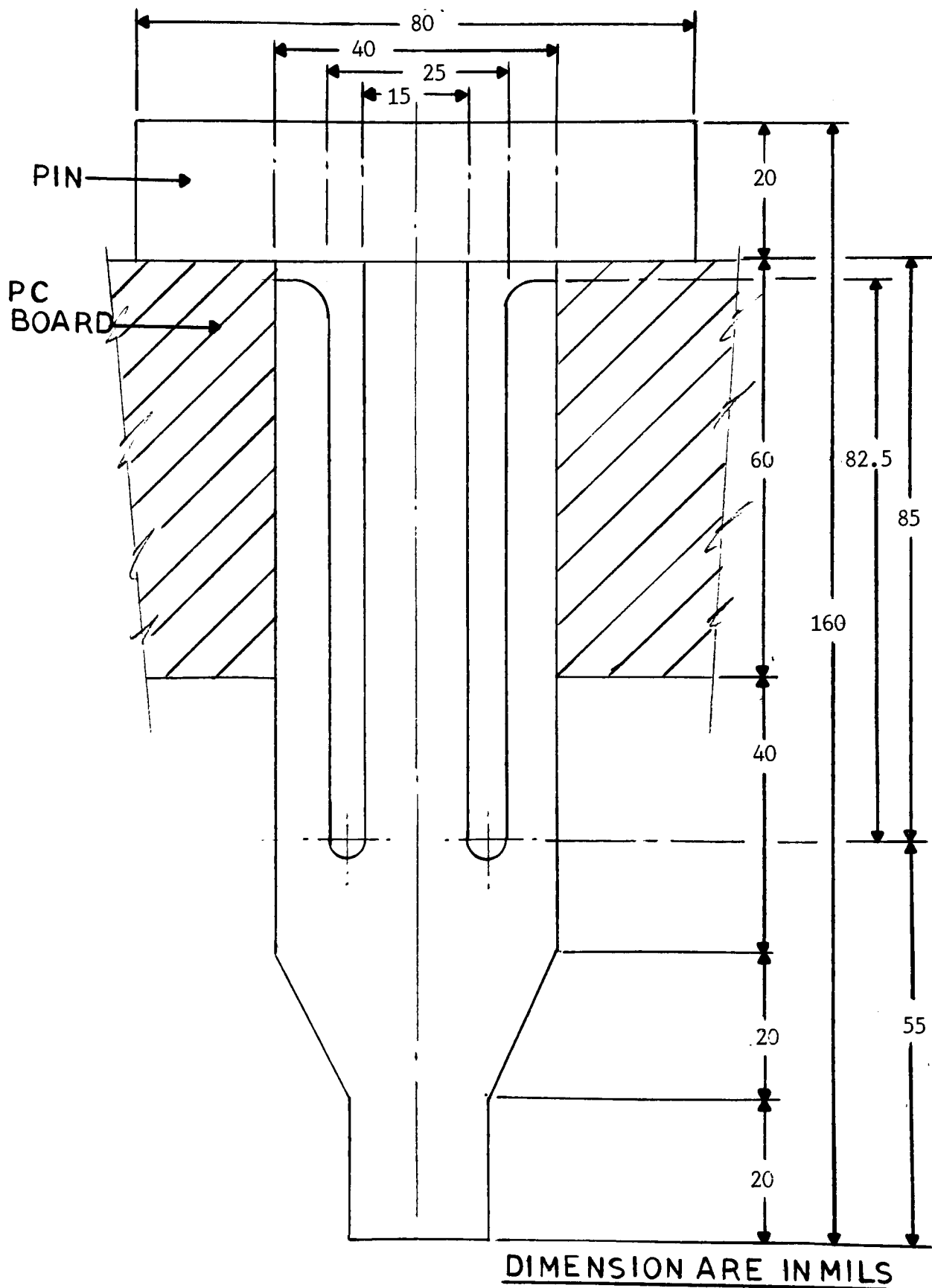numerical models.

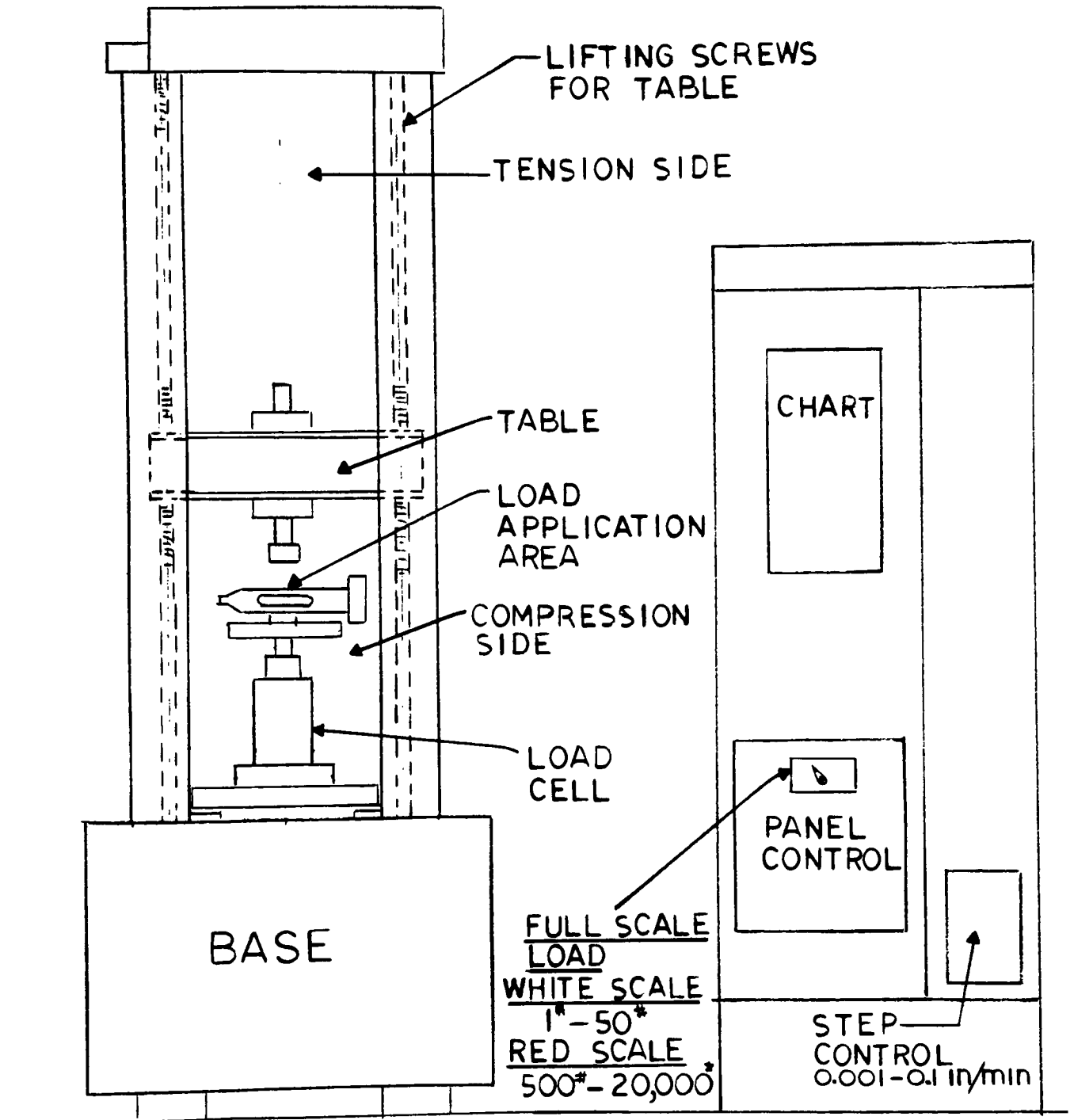Figure  8  Model of Dynamic Retention Pin

Figure 9 Model of Cantilever Pin

Figure 10    Schematic of Instron TTD Machine Showing Model Set-up

# 4. RESULTS AND DISCUSSION

Following are the material parameters of the compliant pins which are used for calculations:

$E = 17 * 10^6$ PSI

$v = 0.28$

$\sigma y = 4.5 * 10^4$ PSI

Hole size = 40 +/- 3 mils

Length of pins = 160 mils

Thickness of PC board = 60 +/- 3 mils

Range of Retention Force = 10 - 25 LBS.

Range of Normal Force = 30 - 75 LBS. (for Coefficient of friction approximately 0.33, Retention Force = Coefficient of friction * Normal Force)

Note : For the cantilever pin, maximum Normal Force = 175 LBS. (Figure 11) which is equivalent to Retention Force of 57 LBS.

The numerical result of Normal Force vs Deflection at load points is shown in Figure 11 for the two compliant pins. For the same range of retention force, in the elastic region, the cantilever pin is more forgiving. As a result, a larger deflection is expected (Figure 12) making the cantilever pin more flexible for different hole sizes in PC boards. A resultant larger deflection would also eliminate loosely fitted pins in PC boards.
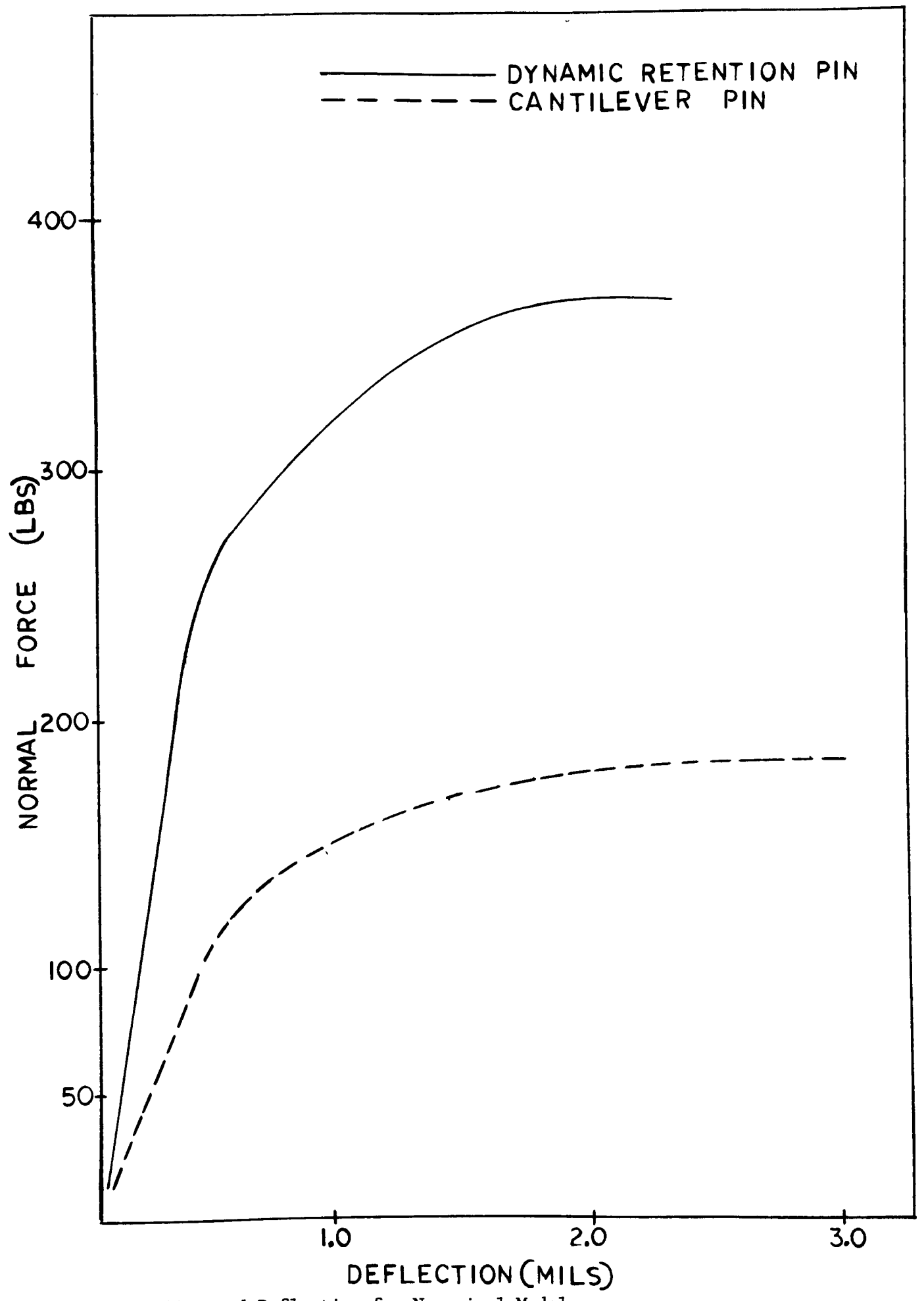
Figure 11  Load Deflection for Numerical Models
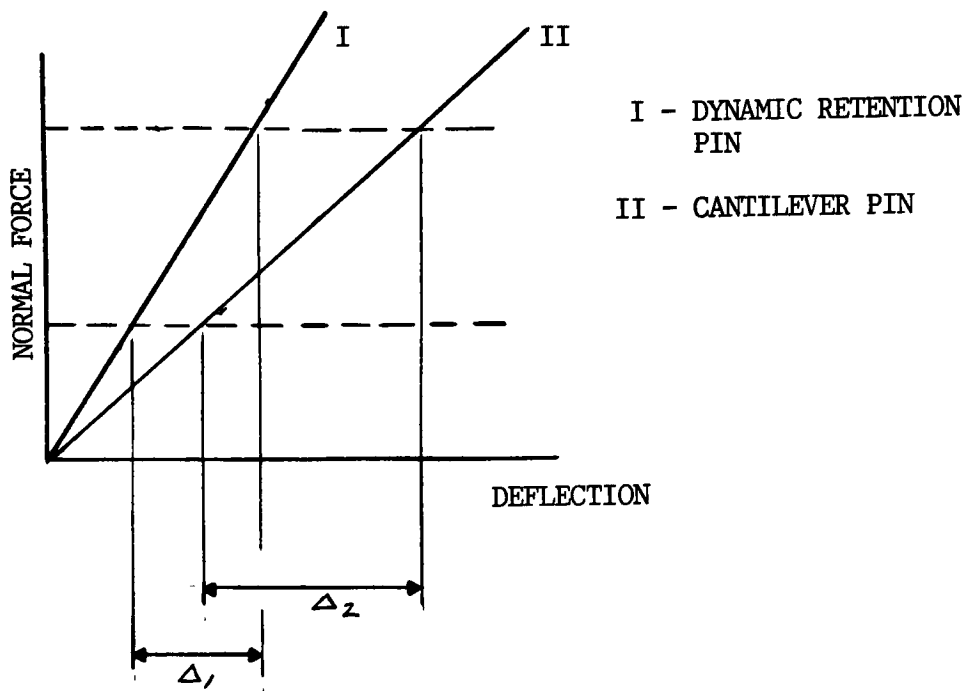
-27-

Figure 12    Effect of the Normal Flexibility of the Pins
             on the amount of Deflection



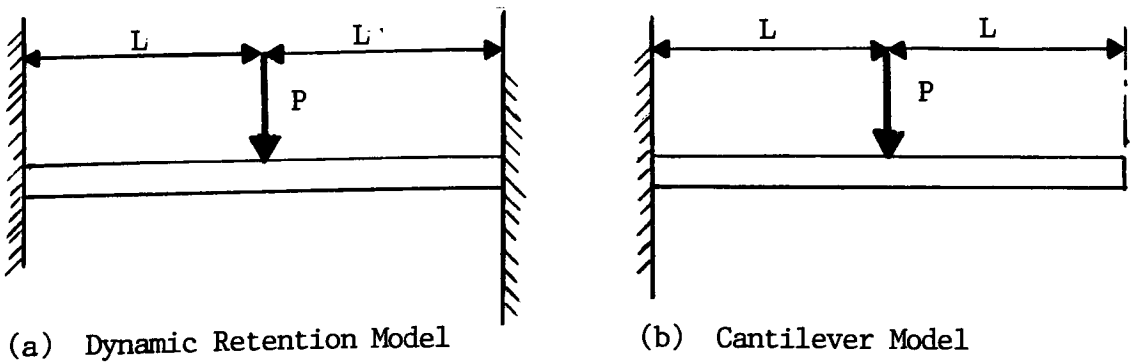(a)  Dynamic Retention Model          (b)  Cantilever Model

Figure 13    Simplified Models of the Two Types of Pins

The propagation of the plastic deformation zone with increasing applied load is depicted in Figures 14 and 15 for both pins. It can be shown that the cantilever pin undergoes more plastic deformation in the transition regions of the compliant part of the pin for the same range of retention force.

The above numerical results agree with the results obtained from simplified models of both pins, a cantilever beam and fixed ends beam (Figure 13). From strength of materials [13,14] the stiffness of the fixed ends and cantilever beams are 24 $EI/L^3$ and 3 $EI/L^3$. Hence, for the same retention force, the cantilever pin is eight times more forgiving. On the other hand, the maximum bending moment for the fixed ends beam is PL/4, which is four times less than that of the cantilever beam, PL. This means that for the same retention force, the cantilever pin undergoes more plastic deformation.

From the experimental results (Figure 16) the cantilever pin model is more forgiving. That is, it has a smaller equivalent stiffness than the dynamic retention pin model. This qualitative analysis compares favorable with the results obtained from the numerical analysis about the flexibility of both pins.
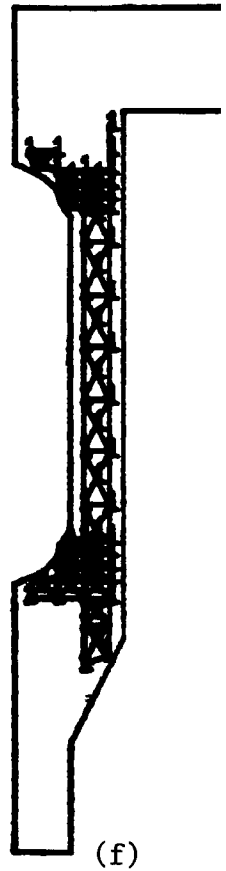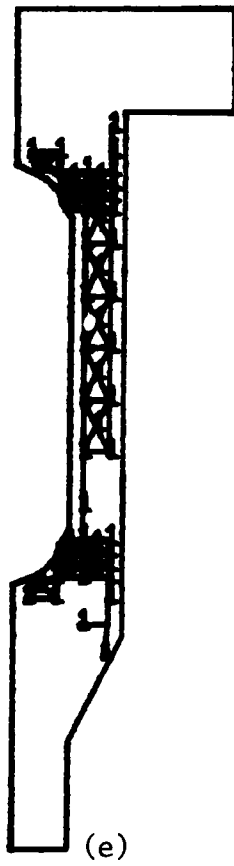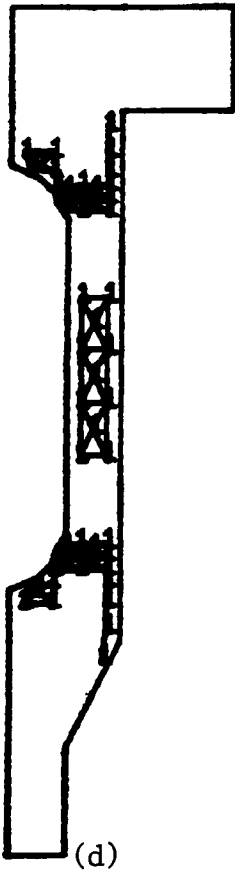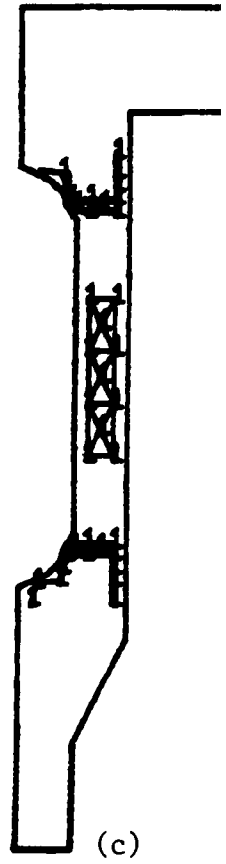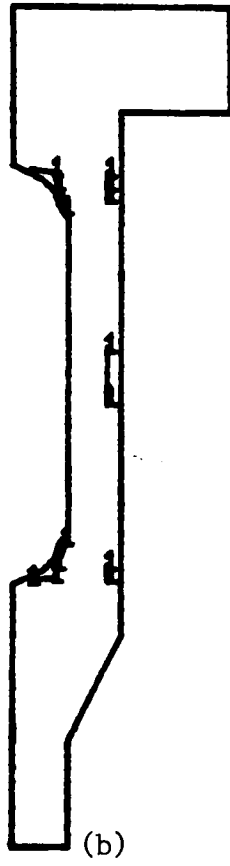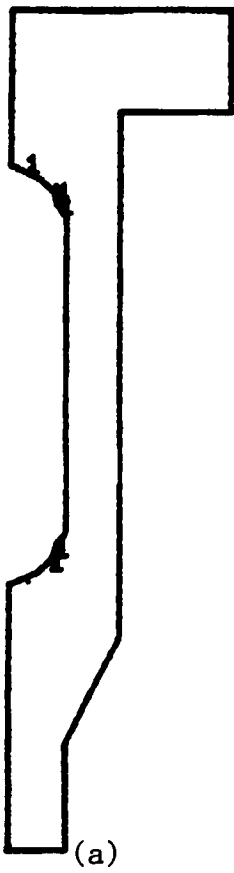
Figure 14    Propagation of Plastic Deformation Zone in
Dynamic Retention Pin at Various Loadings
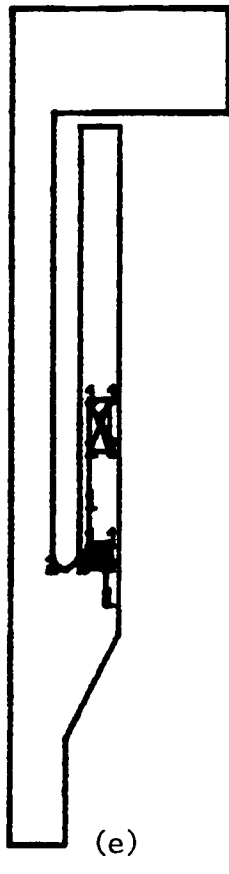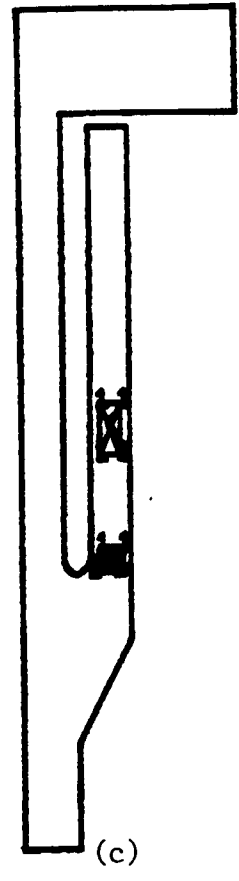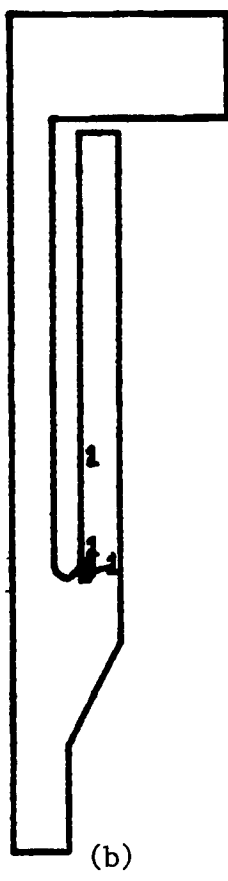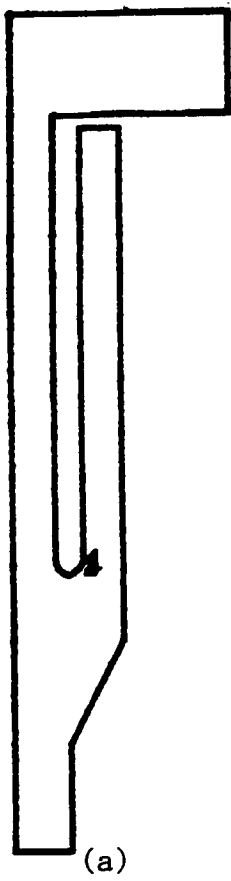
Figure 15    Propagation of Plastic Deformation Zone in
Cantilever Pin at Various Loadings.
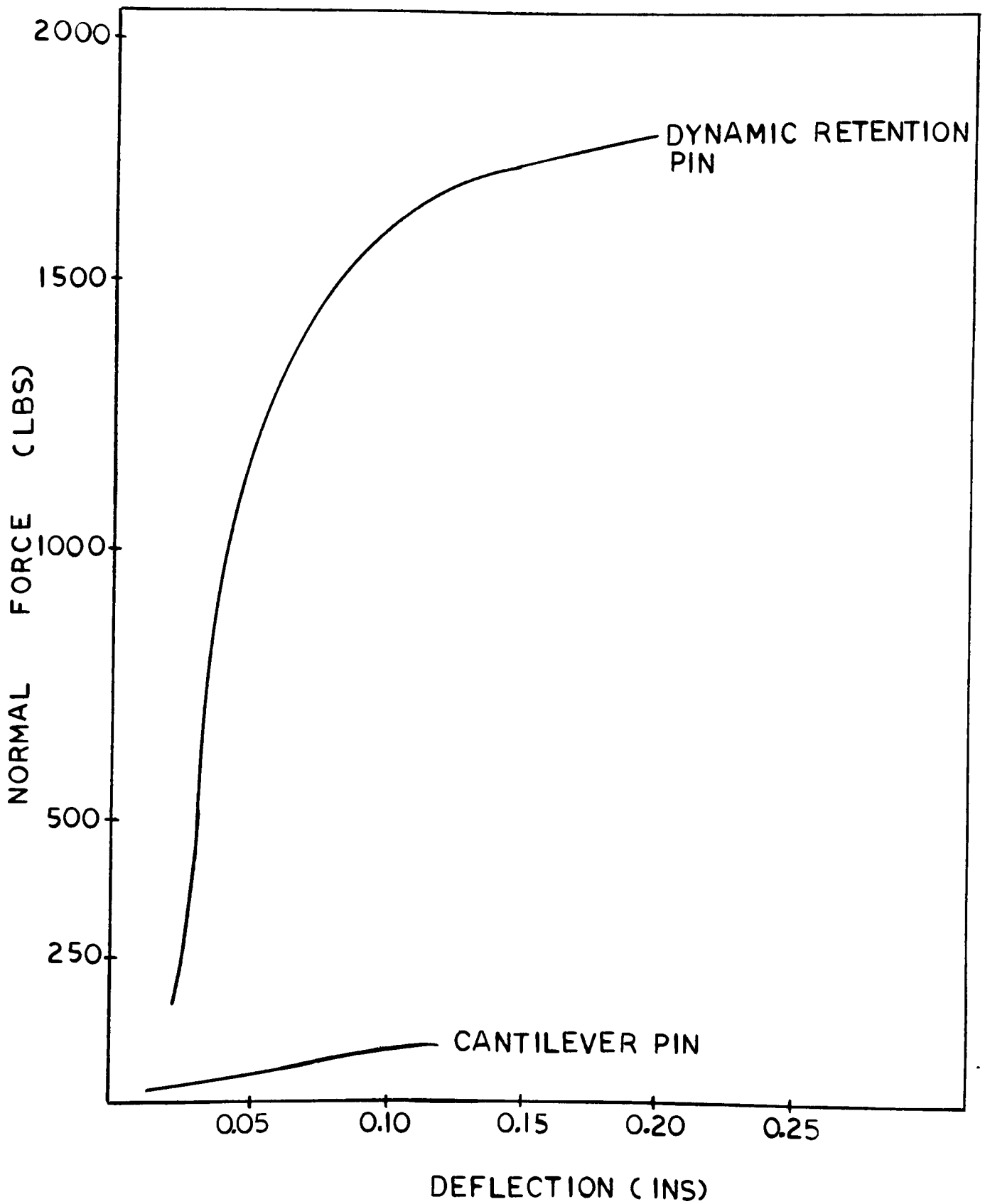
Figure 16   Load Deflection for Experimental Models

# 5. CONCLUSION

From the experimental testing as well as the numerical results it is seen that:

1. The cantilever pin has a smaller stiffness and gives a wider range of deflection for the same range of applied normal force.

2. More plastic deformation occurs in the cantilever pin for the same level of retention force. This implies that the dynamic retention pin (with less plastic deformation) is reliable with both time and frequent replacement.

From a mechanical point of view, the cantilever pin is more advantageous in applications where time and frequent replacement are not factors. For retention forces less than 57 LBS., the cantilever pin has proven to be the better choice for practical applications, since it has a wider range of deflection. On the the other hand, for retention forces over 57 LBS., the dynamic retention pin is still within its elastic range. As a result, it is able to recover and prevent damage to the PC board during the replacement process.

The above analysis implies that there is a trade-off in the utilization of both pins in the PC board industry.

This work can be extended to include creep effect (viscoplasticity) and thermal cyclic effect on the retention forces. Also, parametric analysis can be done to provide optimal dimensions and materials for the pins.

# REFERENCES

1.  R. Geol, "An Analysis of Press Fit Pin Technology",
    Electronic Components Conference, Atlanta Georgia, May 11 -
    13, 1981.

2.  S. M. Ambekar, and I. Farkass ,"Studies On The Performance
    of The Compliant Pins In The Plated Through Hole Of Printed
    Circuit Boards", IPC Fall Meeting, September, 1983, Denver
    Colorado.

3.  R.Cobaugh, and F.Miller, "Compliant Pin An Idea Whose Time
    Has Come", Electronic Component Conference, 1978.

4.  Harry G. Schaeffer, "MSC/NASTRAN Primer", Schaeffer Analysis
    Inc., Mount Vernon, New Hampshire, 1979, pp 76-77.

5.  D. R. J. Owens, and E. Hinton, "Finite Elements In
    Plasticity", Pineridge Press Limited, Swansea, U. K.,1980,
    pp 25-29.

6.  D. R. J. Owens, and E. Hinton, "Finite Elements In
    Plasticity", Pineridge Press Limited, Swansea, U.K., 1980,
    pp 215-229.

7.  A. Mendelson, "Plasticity : Theory And Application", The
    MacMillian Company, New York, 1968, pp 13-14.

8.  MSC/NASTRAN, "Application Manual",  November/December 1984,
    Vol. 1, Section 2.14.

9.  A. C. Ugural, and S. K. Fenster, "Advanced Strength and Applied Elasticity", American Elsevier Publishing Company, New York, 1975, pp 46-68.

10. John K. Krouse, Staff Editor, "Stress Analysis On A Budget", Machine Design, March 8, 1979.

11. A. Mendelson, "Plasticity : Theory And Application", The MacMillian Company, New York, 1968, pp 70-79.

12. J. N. Reddy, "Introduction To The Finite Element Method", McGraw Hill, 1984, pp 265-280.

13. Marks' Standard Handbook For Mechanical Engineers, McGraw-Hill Book Company, 1978, Section 5, pp 24.

14. G.H.Ryder, "Strength of Materials", The MacMillian Press Ltd, London, 1971, pp 175.

15. MSC/NASTRAN, "User Manual", November/December 1984, Vol. 1, Section 2.4, pp 199-218.

16. MSC/NASTRAN, "User Manual", November/December 1984, Vol. 1, Section 2.4, pp 327-330.

17. A. C. Ugural, and S. K. Fenster, "Advanced Strength And Applied Elasticity", American Elsevier Publishing Company, New York, 1975, pp 36-37.

# APPENDIX 1

## STRESS, STRAIN AND ELASTICITY MATRIX
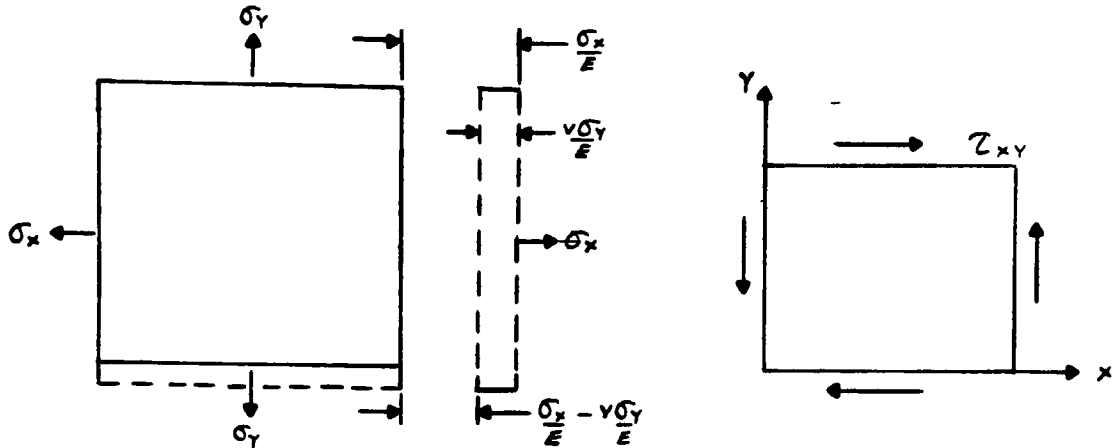


Figure A

From generalized Hooke's Law [9]:

$$E = \frac{\sigma}{\epsilon} \quad \text{(Definition)}$$

From which $\quad \epsilon_x = \dfrac{\sigma_x}{E}$ (A)

For lateral strain in y direction

$$\sigma_y = -\frac{v\,\sigma_x}{E} \tag{B}$$

For a two dimmensional homogenous isotropic element of unit thickness, Figure A, subjected to biaxial stresses, applying the principle of superposition and considering the simultaneous action of $\sigma x$ and $\sigma y$ :

$$\epsilon_x = \frac{\sigma x}{E} - \frac{v\,\sigma y}{E} \tag{C}$$

$$\epsilon y = \frac{\sigma y}{E} - \frac{v \sigma x}{E} \qquad\qquad (D)$$

For pure shear, in the elastic range

$$\gamma_{xy} = \frac{\tau_{xy}}{G} \qquad \text{or} \qquad \tau_{xy} = G\,\gamma_{xy} \qquad\qquad (E)$$

Where $G = \dfrac{E}{2(1+v)}$

Rearranging Equations (C) and (D)

$$\sigma x = E\,\epsilon x + v\,\sigma y \qquad\qquad (F)$$

and

$$\sigma y = E\,\epsilon y + v\,\sigma x \qquad\qquad (G)$$

substituting Equation (G) into Equation (F)

$$\sigma x = E\,\epsilon x + vE\,\epsilon y + v^2 \sigma x$$

simplfying

$$\sigma x(1 - v^2) = E\,(\epsilon x + v\,\epsilon y)$$

$$\text{or} \qquad\qquad \sigma x = \frac{E}{1-v^2}(\epsilon x + v\epsilon_y) \qquad\qquad (H)$$

substituting Equation (F) into Equation (G)

$$\sigma y = E\,\epsilon y + v\,E\,\epsilon x + v^2 \sigma y$$

simplfying and rearranging

$$\sigma y = \frac{E}{1 - v^2}(v\,\epsilon x + \epsilon y) \qquad\qquad (I)$$

writing Equations (E) , (H) and (I) in matrix form :

$$\begin{pmatrix} \sigma x \\ \\ \sigma y \\ \\ \tau xy \end{pmatrix} \begin{matrix} = \\ \\ = \\ \\ = \end{matrix} \begin{bmatrix} \dfrac{E}{1-v^2} & \dfrac{v\,E}{1-v^2} & 0 \\ \\ \dfrac{v\,E}{1-v^2} & \dfrac{E}{1-v^2} & 0 \\ \\ 0 & 0 & \dfrac{E}{2(1+v)} \end{bmatrix} \begin{pmatrix} \epsilon x \\ \\ \epsilon y \\ \\ \gamma xy \end{pmatrix}$$

or

$$\begin{pmatrix} \sigma x \\ \\ \sigma y \\ \\ \tau xy \end{pmatrix} = \begin{bmatrix} D_{11} & D_{12} & 0 \\ \\ D_{21} & D_{22} & 0 \\ \\ 0 & 0 & D_{33} \end{bmatrix} \begin{pmatrix} \epsilon x \\ \\ \epsilon y \\ \\ \gamma xy \end{pmatrix} \tag{J}$$

where $\quad D_{11} = D_{22} = \dfrac{E}{1-v^2} \quad ; \quad D_{12} = D_{21} = \dfrac{v\,E}{1-v^2}$

and $\quad D_{33} = \dfrac{E}{2(1+v)}$

Equation (J) can be written as :

$$\underset{\sim}{\sigma} = [\,D\,]\,\underset{\sim}{\epsilon} \tag{K}$$

# APPENDIX 2

## FORMULATION OF THE FINITE ELEMENT EQUATION

From elasticity theory, displacement method [12]:

Work done by the applied forces = Strain energy

$$\int_{\Omega} u^T \rho \, b \, d\Omega + \int_{\Gamma} u^T \mathcal{T} \, d\Gamma = \int_{\Omega} \frac{1}{2} \epsilon^T \sigma \, d\Omega \qquad (a)$$

Where $\int_{\Omega} u^T \rho \, b \, d\Omega$ is the work done by the body forces

$\int_{\Gamma} u^T \mathcal{T} \, d\Gamma$ is the work done by the surface tractions

$\int_{\Omega} \frac{1}{2} \epsilon^T \sigma \, d\Omega$ is the strain energy

From theory of elasticity [9]:

General strain tensor:

$$\epsilon_{ij} = 1/2 \left( \frac{\partial u_i}{\partial x_j} + \frac{\partial u_j}{\partial x_i} \right)$$

which can be written for plane stress problems as:

$$\epsilon_{xx} = 1/2 \left( \frac{\partial u_x}{\partial x} + \frac{\partial u_x}{\partial x} \right) = \frac{\partial u_x}{\partial x} \qquad (b)$$

$$\epsilon_{yy} = 1/2 \left( \frac{\partial u_y}{\partial y} + \frac{\partial u_y}{\partial y} \right) = \frac{\partial u_y}{\partial y} \qquad (c)$$

The shear strain denoted by $\gamma_{xy}$ is defined as [17]:

$$\gamma_{xy} = \frac{\partial u_x}{\partial y} + \frac{\partial u_y}{\partial x} \qquad (d)$$

writing Equations (b), (c) and (d) in matrix form:

$$\begin{pmatrix} \epsilon_{xx} \\ \epsilon_{yy} \\ \gamma_{xy} \end{pmatrix} = \begin{bmatrix} \dfrac{\partial}{\partial x} & 0 \\ 0 & \dfrac{\partial}{\partial y} \\ \partial\dfrac{\partial}{\partial y} & \partial\dfrac{\partial}{\partial x} \end{bmatrix} \begin{pmatrix} U_x \\ U_y \end{pmatrix}$$

or

$$\underset{\sim}{\epsilon} = [\ L\ ]\ \underset{\sim}{u} \tag{e}$$

From   Equation (K), Appendix 1:

$$\underset{\sim}{\sigma} = [\ D\ ]\underset{\sim}{\epsilon} \tag{f}$$

Combining Equations (e) and (f)

$$\underset{\sim}{\sigma} = [\ D\ ][\ L\ ]\ \underset{\sim}{u} \tag{g}$$

From finite element theory:

$$u = \sum_{i=1}^{N} \psi_i U_i$$

Where    $u$    is the displacement vector

$\psi_i$    is the shape function (linear interpolation

function [12])

$U_i$    nodal displacement value

In two dimensions:

$$\underset{\sim}{U}_x = \sum_{i=1}^{N} \psi_i U_{xi}$$

$$\underset{\sim}{U}_y = \sum_{i=1}^{N} \psi_i U_{yi}$$

In matrix form:

$$\begin{pmatrix} Ux \\ \\ Uy \end{pmatrix} = \begin{bmatrix} \psi_1 & 0 & \psi_2 & 0 \\ \\ 0 & \psi_1 & 0 & \psi_2 \end{bmatrix} \begin{pmatrix} Ux_1 \\ Uy_1 \\ Ux_2 \\ Uy_2 \end{pmatrix}$$

or

$$\underset{\sim}{U} = [\psi]\ \underset{\sim}{U} \tag{h}$$

Combining Equations (h) and (e)

$$\underset{\sim}{\xi} = [L][\psi]\ \underset{\sim}{U}$$

or

$$\underset{\sim}{\xi} = [B]\ \underset{\sim}{U} \tag{i}$$

where [ B ] = Strain/Displacement matrix

Combining Equations (i) and (f)

$$\underset{\sim}{\sigma} = [D][B]\ \underset{\sim}{U} \tag{j}$$

Substituting Equations (h), (i) and (j) into equation (a)

$$\frac{1}{2}\int_{\Omega} \underset{\sim}{U}\ [B]^T[D][B]\underset{\sim}{U}\ d\Omega = \int \underset{\sim}{U}^T\ [\psi]\ \rho\ \underset{\sim}{b}\ d\Omega$$

$$+ \int_{\Gamma} \underset{\sim}{U}^T\ [\psi]^T\ \underset{\sim}{\tau}\ d\Gamma \tag{k}$$

Using the Raleigh-Ritz method, variational functional
I(u) [12]:

$$I(u) = \frac{1}{2}\int \underset{\sim}{U}\ [B]^T[D][B]\underset{\sim}{U}\ d\Omega - \int_{\Omega} \underset{\sim}{U}^T\ [\psi]\rho\ \underset{\sim}{b}\ d\Omega$$

$$- \int_{\Gamma} \underset{\sim}{U}^T [\psi] \underset{\sim}{\tau} d\Gamma \qquad (1)$$

Minimizing $\qquad \dfrac{\partial I(u)}{\partial \psi} = 0$

$$0 = \left( \int_{\Omega} [B]^T [D][B] \, d\Omega \right) \underset{\sim}{U} - \int_{\Omega} [\psi]^T \rho \, \underset{\sim}{b} \, d\Omega$$

$$- \int_{\Gamma} [\psi]^T \underset{\sim}{\tau} \, d\Gamma \qquad (m)$$

Equation (m) can be written as

$$[K] \underset{\sim}{U} = \underset{\sim}{F} \qquad (n)$$

where

$$[K] = \int_{\Omega} [B]^T [D][B] \, d\Omega$$

$$\underset{\sim}{F} = \int_{\Omega} [\psi] \rho \, \underset{\sim}{b} \, d\Omega + \int_{\Gamma} [\psi]^T \underset{\sim}{\tau} \, d\Gamma$$

The force vector F combine the effects of external applied loads and boundary conditions.

# APPENDIX 3

## FORMULATION OF THE ELASTO-PLASTIC MATRIX
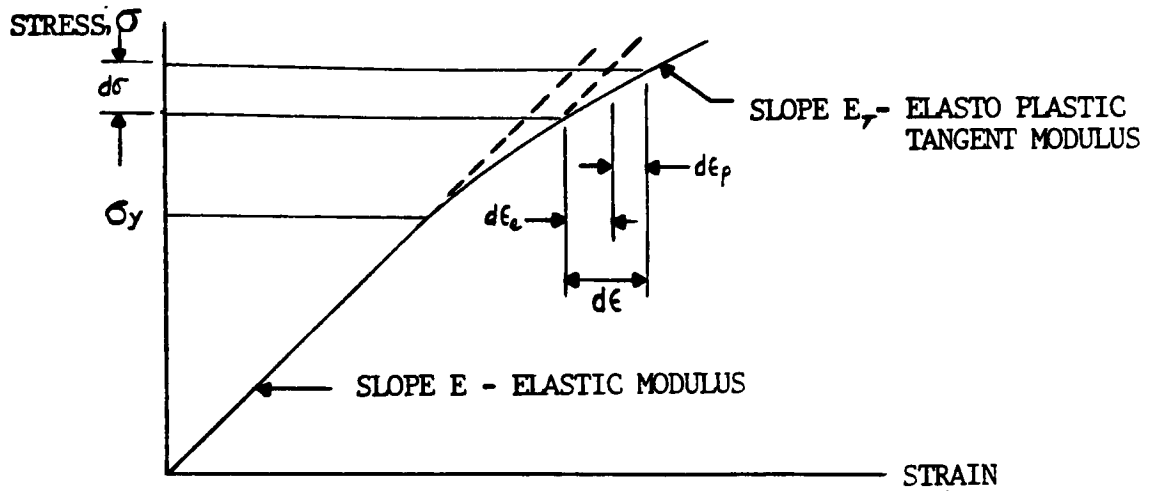


**Figure B   Elasto-Plastic Strain Hardening**

**Behavior For The Uniaxial Case.**

The classical theory of plasticity deals with materials which are elastic until yielding commences at the yield stress $\sigma y$. Thereafter the material response is elasto-plastic with the local tangent to the curve continually varying and is termed the elasto-plastic Tangent Modulus, $E_T$ which is a function of strain.

The progressive development of the yield surface can be defined by relating the yield stress, $\sigma y$, to the plastic deformation by means of the hardening parameter k [6].

$$k = W_p \tag{a}$$

Where $W_p$ is the plastic work

$$W_p = \int \sigma_{ij} (d\epsilon_{ij})_p \tag{b}$$

in which $(d\epsilon_{ij})_p$ are the plastic components of the strain occuring during a strain increment.

The effective or equivalent plastic strain is defined incrementally as:

$$d\bar{\epsilon}_p = \sqrt{\tfrac{2}{3}} \{ (d\epsilon_{ij})_p (d\epsilon_{ij})_p \} \tag{c}$$

For situations where the assumption that yielding is independent of any hydrostatic stress is valid, $(d\epsilon_{ij})_p = 0$ and hence $(d\epsilon_{ij}')_p = (d\epsilon_{ij})_p$

Equation (c) can be written as:

$$d\bar{\epsilon}_p = \sqrt{\tfrac{2}{3}} \{ (d\epsilon_{ij}')_p (d\epsilon_{ij}')_p \} \tag{d}$$

Then the hardening parameter, k, is assumed to be defined as:

$$k = \bar{\epsilon}_p \tag{e}$$

where $\bar{\epsilon}_p$ is the result of integrating $d\bar{\epsilon}_p$ over the strain path.

Also, the strain hardening parameter $H'$, is defined as

$$H' = \frac{d\sigma}{d\epsilon_p} \tag{f}$$

Using Equation (e), equation (f) can be written in terms of the effective stress, $\bar{\sigma}$ :

$$\bar{\sigma} = H (p) \tag{g}$$

or differentiating

$$\frac{d\bar{\sigma}}{d\bar{\epsilon}p} = H'(\bar{\epsilon}p) \qquad \text{(h)}$$

For the uniaxial case $\sigma_1 = \sigma$, $\sigma_2 = \sigma_3 = 0$ and thus from effective stress $\bar{\sigma} = \sqrt{\frac{3}{2}} \{ \sigma_{ij}' \sigma_{ij}' \}^{\frac{1}{2}}$
we have [6]:

$$\bar{\sigma} = \sigma \qquad \text{(i)}$$

If the plastic strain increment in the direction of loading is $d\epsilon p$, then $(d\epsilon_1)p = d\epsilon p$ and since plastic straining is assumed to be incompressible, poissons's ratio is effectively 0.5 and $(d\epsilon_2)p = \frac{1}{2} d\epsilon p$ and $(d\epsilon_3)p = -\frac{1}{2} d\epsilon p$. Then from Equation (c) the effective plastic strain becomes:

$$d\bar{\epsilon}p = \sqrt{\frac{2}{3}} \{ (\epsilon_{ij}')p (\epsilon_{ij}')p \}^{\frac{1}{2}} = d\epsilon p \qquad \text{(j)}$$

Using Equations (i) and (j) then Equation (h) becomes

$$H'(\bar{\epsilon}p) = \frac{d\sigma}{d\epsilon_p} = \frac{d\sigma}{d\epsilon - d\epsilon_e} = \frac{1}{\frac{d\epsilon}{d\sigma} - \frac{d\epsilon_e}{d\sigma}}$$

where $d\epsilon = d\epsilon_e + d\epsilon_p$ (From Figure B)

$$\text{or} \qquad H' = \frac{E_T}{1 - \frac{E_T}{E}} \qquad \text{(k)}$$

$H'$ can be determined experimentally from a simple uniaxial test.

The yield function at which plastic deformation begins can be written in the general form

$$f\ (\underset{\sim}{\sigma})\ =\ K\ (\ k\ ) \tag{1}$$

Where $\underset{\sim}{\sigma}$ is the stress vector and $k$ is the hardening parameter.

From Equations (a) and (b)

$$dk\ =\ \underset{\sim}{\sigma}^T d\ \underset{\sim}{\epsilon}\,p$$

and $\quad dk\ =\ d\underset{\sim}{\epsilon}p \qquad$ from Equationn (e)

Rearranging Equation (1)

$$F\ (\ \underset{\sim}{\sigma}\ ,\ k\ )\ =\ f\ (\underset{\sim}{\sigma})\ -\ K\ (k)\ =\ 0 \tag{m}$$

By differentiating Equation (m)

$$dF\ =\ \frac{\partial F}{\partial \underset{\sim}{\sigma}}\ d\underset{\sim}{\sigma}\ +\ \frac{\partial F}{\partial \kappa}\ d\kappa\ =\ 0 \tag{n}$$

or

$$\underset{\sim}{a}^T d\sigma\ -\ A\ d\lambda\ =\ 0 \tag{o}$$

with the definitions:

$$\underset{\sim}{a}^T\ =\ \frac{\partial F}{\partial \sigma}\ =\ \left[\ \frac{\partial F}{\partial \sigma x}\ ,\ \frac{\partial F}{\partial \sigma y},\ \frac{\partial F}{\partial \sigma z},\ \frac{\partial F}{\partial \tau yz},\ \frac{\partial F}{\partial \tau zx},\ \frac{\partial F}{\partial \tau xy}\ \right] \tag{p}$$

and $\quad A\ =\ -\ \dfrac{1}{d\lambda}\ \dfrac{\partial F}{\partial \kappa}\ d\kappa \tag{q}$

The vector $\underset{\sim}{a}$ is termed the flow vector.

The incremental relationship between stress and strain for elasto-plastic deformation is defined as [6]:

$$d\epsilon_{ij} = \frac{d\sigma_{ij}}{2\mu} + \frac{(1 - 2v)}{E} \delta_{ij}\, d\sigma_{\kappa\kappa} + d\lambda \frac{\delta f}{\delta \sigma_{ij}} \qquad (r)$$

Equation (r) can be written as:

$$d\underset{\sim}{\epsilon} = [D]^{-1}\, d\underset{\sim}{\sigma} + d\lambda \frac{\delta F}{\delta \underset{\sim}{\sigma}} \qquad (s)$$

where [D] is the matrix of elastic constants (Appendix 1)
Pre-multiplying Equation (s) by $\underset{\sim}{d}D^{T} = \underset{\sim}{a}^{T}[D]$ and eliminating $\underset{\sim}{a}^{T}\, d\sigma$ by using Equation (o), the plastic multiplier:

$$d\lambda = \frac{1}{A + \underset{\sim}{a}^{T}[D]\underset{\sim}{a}}\underset{\sim}{a}^{T}\, dD\, d\underset{\sim}{\epsilon} \qquad (t)$$

Substituting Equation (t) into Equation (s)

$$d\underset{\sim}{\sigma} = [Dep]\, d\underset{\sim}{\epsilon}$$

with $[Dep] = [D] - \dfrac{\underset{\sim}{d}D\, \underset{\sim}{d}D^{T}}{A + \underset{\sim}{d}^{T}\underset{\sim}{a}}; \quad \underset{\sim}{d}D = [D]\underset{\sim}{a} \qquad (u)$

Where [Dep] is the Elasto-Plastic matrix

Stiffness matrix (from Equation (n), Appendix 2)

$$[K] = \int_{\underline{\Omega}} [B]^{T}[Dep][B]\, d\Omega \qquad (v)$$

Which shows that the non-linearities occur in [K].

```
*****************************************************
*
*  PROGRAM          :  MSC/NASTRAN SOLUTION 66
*                      NON - LINEAR ANALYSIS
*
*  PROGRAMMER       :  LINCOLN  G. MILLER
*
*  DATE WRITTEN     :  DEC. 17,1985
*
*  OBJECTIVE        :  TO STUDY THE CANTILEVER PIN
*                      (COMPLINT PIN) SUBJECTED TO
*                      PLASTIC DEFORMATION.
*
*****************************************************

ID MILLER,LG
TIME 60
SCL 66
CEND
TITLE = CANTILEVER PIN PROBLEM
SUBTITLE =COMPLIANT PIN
SPC = 100
SEALL = ALL
STRESS = ALL
DISP = ALL
SPCFORCE = ALL
SUBCASE 1
LOAD = 10
NLPARM = 10
SUBCASE 2
LOAD = 20
NLPARM = 20
SUBCASE 3
LOAD = 30
NLPARM = 30
OUTPUT(PLOT)
PLOTTER NASTRAN
CSCALE 2.2
PAPER SIZE 26. X 20.
SET 1 = ALL
AXES Z,X,Y
VIEW 0.,0.,0.
MAXI DEFO 0.000001
FIND SCALE,SET 1,ORIGIN 1
PLOT SET 1,ORIGIN 1,LABEL GRID POINTS
PLOT SET 1,ORIGIN 1,LABEL ELEMENTS
PLOT SET 1,ORIGIN 1,SHRINK
PLOT STATIC DEFO 0,1 SET 1,ORIGIN 1
CONTOUR MAXSHEAR LIST 4.5+4
PLOT CONTOUR  SET 1 ORIGIN 1 OUTLINE
CONTOUR MAXSHEAR LIST 4.4+4
PLOT CONTOUR  SET 1 ORIGIN 1 OUTLINE
BEGIN BULK
PARAM,SUBID,3
PARAM,LOADINC,4
PARAM,LOOPID,24
GRDSET,,,,,,,3456
GRID,1,,0.0,0.060,0.0
GRID,2,,0.0,0.060,0.0
GRID,3,,0.0,0.050,0.0
```

-49-

```
GRID,4,,0.0,0.040,0.0
GRID,5,,0.0,0.030,0.0
GRID,6,,0.0,0.020,0.0
GRID,7,,0.0,0.01,0.0
GRID,8,,0.0,0.0,0.0
GRID,9,,0.0,-0.010,0.0
GRID,10,,0.0,-0.020,0.0
GRID,11,,00,-0.0275,0.0
GRID,12,,0.0,-0.040,0.0
GRID,13,,0.0,-0.050,0.0
GRID,14,,0.0,-0.060,0.0
GRID,15,,0.0,-0.070,0.0
GRID,16,,0.0,-0.080,0.0
GRID,17,,0.010,-0.080,0.0
GRID,18,,0.010,-0.070,0.0
GRID,19,,0.010,-0.060,0.0
GRID,20,,0.015,-0.050,0.0
GRID,21,,0.020,-0.040,0.0
GRID,22,,0.020,-0.0275,0.0
GRID,23,,0.020,-0.020,0.0
GRID,24,,0.02,-0.010,0.0
GRID,25,,0.020,0.0,0.0
GRID,26,,0.020,0.01,0.0
GRID,27,,0.020,0.020,0.0
GRID,28,,0.020,0.030,0.0
GRID,29,,0.020,0.040,0.0
GRID,30,,0.020,0.050,0.0
GRID,31,,0.020,0.0575,0.0
GRID,32,,0.020,0.060,0.0
GRID,33,,0.040,0.060,0.0
GRID,34,,0.040,0.050,0.0
GRID,35,,0.020,0.050,0.0
GRID,36,,0.0075,0.050,0.0
GRID,37,,0.0075,0.06,0.0
GRID,38,,0.0075,0.05,0.0
GRID,39,,0.0075,0.040,0.0
GRID,40,,0.0075,0.030,0.0
GRID,41,,0.0075,0.020,0.0
GRID,42,,0.0075,0.010,00
GRID,43,,0.0075,0.0,0.0
GRID,44,,0.0075,-0.01,0.0
GRID,45,,0.0075,-0.020,0.0
GRID,48,,0.0125,-0.02,0.0
GRID,49,,0.0125,-0.010,0.0
GRID,50,,0.0125,0.0,0.0
GRID,51,,0.0125,0.010,0.0
GRID,52,,0.0125,0.02,0.0
GRID,53,,0.0125,0.03,0.0
GRID,54,,0.0125,0.04,0.0
GRID,55,,0.0125,0.05,0.0
GRID,56,,0.0125,0.0575,0.0
GRID,60,,0.010,-0.040,0.0
GRID,61,,0.010,-0.0275,0.0
GRID,62,,0.0075,-0.025,0.0
GRID,63,,0.0125,-0.025,0.0
GRID,64,,0.011875,-0.02625,0.0
GRID,65,,0.008125,-0.02625,0.0
GRID,66,,0.00875,-0.02583,0.0
GRID,67,,0.01125,-0.02683,0.0
GRID,68,,0.009375,-0.0273,0.0
```

```
GRID,69,,0.010625,-0.0273,C.0
GRID,70,,0.02,-0.0265,0.0
GRID,71,,0.02,-0.026,0.0
GRID,72,,0.02,-0.0255,0.0
GRID,73,,0.02,-0.025,0.0
GRID,74,,0.0,-0.025,0.0
GRID,75,,0.0,-0.0255,0.0
GRID,76,,0.0,-0.026,0.0
GRID,77,,0.0,-0.0265,C.0
GRID,78,,0.00375,0.08,0.0
GRID,79,,0.00375,0.06,0.0
GRID,80,,0.00375,0.05,0.0
GRID,81,,0.00375,0.04,0.0
GRID,82,,0.00375,0.03,0.0
GRID,83,,0.00375,0.02,0.0
GRID,84,,0.00375,0.010,0.0C
GRID,85,,0.00375,0.0,0.0
GRID,86,,0.00375,-0.01,0.0
GRID,87,,0.00375,-0.020,0.0
GRID,88,,0.00375,-0.025,0.0
GRID,89,,0.004,-0.0255,C.C
GRID,90,,0.00425,-0.026,0.0
GRID,91,,0.0045,-0.0265,0.0
GRID,92,,0.005,-0.0275,C.0
GRID,93,,0.005,-0.04,0.0
GRID,94,,0.005,-0.05,C.0
GRID,95,,0.005,-0.06,0.C
GRID,96,,0.005,-0.07,0.C
GRID,97,,0.005,-0.08,0.0
GRID,98,,0.01,-0.05,0.0
GRID,99,,0.015,-0.040,0.0
GRID,100,,0.015,-0.0275,0.0
GRID,101,,0.0155,-0.0255,0.0
GRID,102,,0.01575,-0.026,C.0
GRID,103,,0.015,-0.0255,0.0
GRID,104,,0.01525,-0.025,0.0
GRID,105,,0.01525,-0.02,0.0
GRID,106,,0.01625,-0.01,0.0
GRID,107,,0.01625,0.0,0.0
GRID,108,,0.01625,0.01,0.0
GRID,109,,0.01625,0.02,0.0
GRID,110,,0.01625,0.03,0.0
GRID,111,,0.01625,0.04,0.0
GRID,112,,0.01625,0.05,0.0
GRID,113,,0.01625,0.0575,C.0
CQUAD4,1,50,16,97,96,15
CQUAD4,2,50,97,17,18,96
CQUAD4,3,50,15,96,95,14
CQUAD4,4,50,96,18,19,95
CQUAD4,5,50,14,95,94,13
CTRIA3,6,50,95,98,94
CQUAD4,7,50,95,19,20,93
CQUAD4,8,50,13,94,93,12
CQUAD4,9,50,94,93,60,93
CTRIA3,10,50,93,99,60
CQUAD4,11,50,93,20,21,99
CQUAD4,12,50,12,93,92,11
CQUAD4,13,50,93,60,61,92
CQUAD4,14,50,60,99,100,61
CQUAD4,15,50,99,21,22,100
```

```
CQUAD4,16,50,11,92,91,77
CQUAD4,17,50,92,61,68,91
CQUAD4,18,50,77,91,90,76
CQUAD4,19,50,91,68,66,90
CQUAD4,20,50,76,90,89,75
CQUAD4,21,50,90,66,65,89
CQUAD4,22,50,75,89,88,74
CQUAD4,23,50,89,65,62,88
CQUAD4,24,50,61,100,101,69
CQUAD4,25,50,100,22,70,101
CQUAD4,26,50,69,101,102,67
CQUAD4,27,50,101,70,71,102
CQUAD4,28,50,67,102,103,64
CQUAD4,29,50,102,71,72,103
CQUAD4,30,50,64,103,104,63
CQUAD4,31,50,103,72,73,104
CQUAD4,32,50,74,88,87,10
CQUAD4,33,50,88,62,45,87
CQUAD4,34,50,10,87,86,9
CQUAD4,35,50,87,45,44,86
CQUAD4,36,50,9,86,85,8
CQUAD4,37,50,86,44,43,85
CQUAD4,38,50,8,85,84,7
CQUAD4,39,50,85,43,42,84
CQUAD4,40,50,7,84,83,6
CQUAD4,41,50,84,42,41,83
CQUAD4,42,50,6,83,82,5
CQUAD4,43,50,83,41,40,82
CQUAD4,44,50,5,82,81,4
CQUAD4,45,50,82,40,39,81
CQUAD4,46,50,4,81,80,3
CQUAD4,47,50,81,39,38,80
CQUAD4,48,50,3,80,79,2
CQUAD4,49,50,80,38,37,79
CQUAD4,50,50,2,79,78,1
CQUAD4,51,50,79,37,36,78
CQUAD4,52,50,37,32,35,36
CQUAD4,53,50,32,33,34,35
CQUAD4,54,50,63,104,105,48
CQUAD4,55,50,104,73,23,105
CQUAD4,56,50,48,105,106,49
CQUAD4,57,50,105,23,24,106
CQUAD4,58,50,49,106,107,50
CQUAD4,59,50,106,24,25,107
CQUAD4,60,50,50,107,108,51
CQUAD4,61,50,107,25,26,108
CQUAD4,62,50,51,108,109,52
CQUAD4,63,50,108,26,27,109
CQUAD4,64,50,52,109,110,53
CQUAD4,65,50,109,27,28,110
CQUAD4,66,50,53,110,111,54
CQUAD4,67,50,110,28,29,111
CQUAD4,68,50,54,111,112,55
CQUAD4,69,50,111,29,30,112
CQUAD4,70,50,55,112,113,56
CQUAD4,71,50,112,30,31,113
PSHELL,50,40,1.0,40
MAT1,40,1.7+7,,0.28
MATS1,40,,PLASTIC,0.0,1,1,4.5+4
SPC1,100,1,1,THRU,16
```

```
SPC1,100,1,74,75,76,77
SPC1,100,2,1
SPC1,100,1,25,26
SPCD,10,25,1,-0.00065
SPCD,10,26,1,-0.00065
SPCD,20,25,1,-0.0015
SPCD,20,26,1,-0.0015
SPCD,30,25,1,-0.003
SPCD,30,26,1,-0.003
FORCE,10,25,,0.00,-1.0,0.0,0.0
FORCE,10,26,,0.00,-1.0,0.0,0.0
FORCE,20,25,,0.00,-1.0,0.0,0.0
FORCE,20,26,,0.00,-1.0,0.0,0.0
FORCE,30,25,,0.00,-1.0,0.0,0.0
FORCE,30,26,,0.00,-1.0,0.0,0.0
GRID,270,,0.020,0.020,0.0,,123456
GRID,280,,0.02,0.030,0.0,,123456
GRID,290,,0.020,0.04,0.0,,123456
GRID,300,,0.020,0.05,0.0,,123456
GRID,310,,0.020,0.0575,0.0,,123456
CGAP,270,43,27,270,,,,0
CGAP,280,53,28,280,,,,0
CGAP,290,63,29,290,,,,0
CGAP,300,73,30,300,,,,0
CGAP,310,83,31,310,,,,0
PGAP,43,0.0043,0.043,1.0+6,1.0+1,1.-8
PGAP,53,0.0053,0.053,1.0+6,1.0+1,1.-8
PGAP,63,0.0063,0.063,1.0+6,1.0+1,1.-8
PGAP,73,0.0073,0.073,1.0+6,1.0+1,1.-8
PGAP,83,0.0083,0.083,1.0+6,1.0+1,1.-8
NLPARM,10,5,,AUTO,,,W,YES
NLPARM,20,15,,AUTO,,,W,YES
NLPARM,30,5,,AUTO,,,W,YES
ENDDATA
```

```
******************************************************
*
*  PROGRAM        : MSC/NASTRAN SOLUTION 66
*                   NON - LINEAR ANALYSIS
*
*  PROGRAMMER     : LINCOLN G. MILLER
*
*  DATE WRITTEN : DEC. 17, 1985
*
*  OBJECTIVE      : TO STUDY THE DYNAMIC RETENTION
*                   PIN(COMPLIANT PIN) SUBJECTED TO
*                   PLASTIC DEFORMATION.
*
******************************************************
ID MILLER,LG
TIME 50
SOL 66
CEND
TITLE = DYNAMIC RETENTION PIN PROBLEM
SUBTITLE = COMPLIANT PIN
SPC = 100
SEALL = ALL
STRESS = ALL
DISP = ALL
SPCFORCE = ALL
SUBCASE 1
LOAD = 10
NLPARM = 10
SUBCASE 2
LOAD = 20
NLPARM = 20
SUBCASE 3
LOAD = 30
NLPARM =30
OUTPUT(PLOT)
PLOTTER NASTRAN
CSCALE 2.2
PAPER SIZE 26. X 20.
SET 1 = ALL
AXES Z,X,Y
VIEW 0.,0.,0.
MAXI DEFO 0.000001
FIND SCALE,SET 1,ORIGIN 1
PLOT SET 1,ORIGIN 1,LABEL GRID POINTS
PLOT SET 1,ORIGIN 1,LABEL ELEMENTS
PLOT SET 1,ORIGIN 1,SHRINK
PLOT STATIC DEFO 0, SET 1,ORIGIN 1
CONTOUR MAXSHEAR LIST 4.5+4
PLOT CONTOUR  SET 1 ORIGIN 1 OUTLINE
CONTOUR MAXSHEAR LIST 4.4+4
PLOT CONTOUR  SET 1 ORIGIN 1 OUTLINE
BEGIN BULK
PARAM,SUBID,2
PARAM,LOADINC,20
PARAM,LOOPID,25
GRDSET,,,,,,,3456
GRID,1,,0.0,-0.050,0.0
GRID,2,,0.0,-0.050,0.0
```

-54-

```
GRID,3,,0.0,-0.040,0.0
GRID,4,,0.0,-0.030,0.0
GRID,5,,0.005,-0.0275,0.0
GRID,6,,0.0075,-0.025,0.0
GRID,7,,0.0085,-0.0225,0.0
GRID,8,,0.010,-0.020,0.0
GRID,9,,0.010,-0.010,0.0
GRID,10,,0.010,0.0,0.0
GRID,11,,0.010,0.010,0.0
GRID,12,,0.010,0.020,0.0
GRID,13,,0.010,0.030,0.0
GRID,14,,0.010,0.040,0.0
GRID,15,,0.0085,0.0425,0.0
GRID,16,,0.0075,0.045,0.0
GRID,17,,0.005,0.0475,0.0
GRID,18,,0.00,0.050,0.0
GRID,19,,0.00,0.060,0.0
GRID,20,,0.00,0.060,0.0
GRID,21,,0.020,0.080,0.0
GRID,22,,0.040,0.030,0.0
GRID,23,,0.040,0.060,0.0
GRID,24,,0.020,0.060,0.0
GRID,25,,0.020,0.050,0.0
GRID,26,,0.020,0.0475,0.0
GRID,27,,0.020,0.045,0.0
GRID,28,,0.020,0.0425,0.0
GRID,29,,0.020,0.040,0.0
GRID,30,,0.020,0.030,0.0
GRID,31,,0.020,0.020,0.0
GRID,32,,0.020,0.010,0.0
GRID,33,,0.020,0.00,0.0
GRID,34,,0.020,-0.010,0.0
GRID,35,,0.020,-0.020,0.0
GRID,36,,0.020,-0.0225,0.0
GRID,37,,0.020,-0.025,0.0
GRID,38,,0.020,-0.0275,0.0
GRID,39,,0.020,-0.030,0.0
GRID,40,,0.020,-0.040,0.0
GRID,41,,0.010,-0.060,0.0
GRID,42,,0.010,-0.080,0.0
GRID,50,,0.0,-0.050,0.0
GRID,51,,0.005,-0.050,0.0
GRID,52,,0.010,-0.05,0.0
GRID,53,,0.015,-0.050,0.0
GRID,54,,0.015,-0.040,0.0
GRID,55,,0.010,-0.040,0.0
GRID,56,,0.005,-0.040,0.0
GRID,57,,0.0,-0.035,0.0
GRID,58,,0.005,-0.035,0.0
GRID,59,,0.010,-0.035,0.0
GRID,60,,0.015,-0.035,0.0
GRID,61,,0.020,-0.035,0.0
GRID,62,,0.005,-0.030,0.0
GRID,63,,0.010,-0.030,0.0
GRID,64,,0.015,-0.030,0.0
GRID,65,,0.015,-0.0275,0.0
GRID,66,,0.010,-0.0275,0.0
GRID,67,,0.010,-0.025,0.0
GRID,68,,0.015,-0.025,0.0
GRID,69,,0.015,-0.0225,0.0
```

```
GRID,70,,0.010,-0.0225,0.0
GRID,71,,0.015,-0.020,0.0
GRID,72,,0.015,-0.010,0.0
GRID,73,,0.015,0.0,0.0
GRID,74,,0.015,0.010,0.0
GRID,75,,0.015,0.020,0.0
GRID,76,,0.015,0.030,0.0
GRID,77,,0.015,0.040,0.0
GRID,78,,0.015,0.0425,0.0
GRID,79,,0.010,0.0425,0.0
GRID,80,,0.010,0.045,0.0
GRID,81,,0.015,0.045,0.0
GRID,82,,0.015,0.0475,0.0
GRID,83,,0.010,0.0475,0.0
GRID,84,,0.005,0.050,0.0
GRID,85,,0.010,0.050,0.0
GRID,86,,0.015,0.050,0.0
GRID,87,,0.015,0.055,0.0
GRID,88,,0.010,0.055,0.0
GRID,89,,0.005,0.055,0.0
GRID,90,,0.0,0.055,0.0
GRID,91,,0.005,0.05,0.0
GRID,92,,0.010,0.060,0.0
GRID,93,,0.015,0.060,0.0
GRID,94,,0.015,0.050,0.0
GRID,95,,0.010,0.050,0.0
GRID,96,,0.005,0.030,0.0
GRID,97,,0.020,0.055,0.0
GRID,98,,0.005,-0.080,0.0
GRID,99,,0.005,-0.060,0.0
CQUAD4,1,50,1,98,99,2
CQUAD4,2,50,98,42,41,99
CQUAD4,3,50,2,99,51,50
CQUAD4,4,50,99,41,52,51
CTRIA3,30,50,41,53,52
CQUAD4,5,50,50,51,56,3
CQUAD4,6,50,51,52,55,56
CQUAD4,7,50,52,53,54,55
CTRIA3,31,50,53,40,54
CQUAD4,8,50,3,56,58,57
CQUAD4,9,50,56,55,59,58
CQUAD4,10,50,55,54,60,59
CQUAD4,11,50,54,40,61,60
CQUAD4,12,50,57,58,62,4
CQUAD4,13,50,58,59,63,62
CQUAD4,14,50,59,60,64,63
CQUAD4,15,50,60,61,39,64
CTRIA3,32,50,4,62,5
CQUAD4,16,50,62,63,65,5
CQUAD4,17,50,63,64,65,66
CQUAD4,18,50,64,39,36,65
CQUAD4,19,50,5,66,67,6
CQUAD4,20,50,66,65,66,67
CQUAD4,21,50,65,38,37,66
CQUAD4,22,50,6,67,70,7
CQUAD4,23,50,67,68,69,70
CQUAD4,24,50,66,37,36,69
CTRIA3,25,50,7,70,8
CQUAD4,26,50,70,69,71,8
CQUAD4,27,50,69,36,35,71
```

```
CQUAD4,28,50,8,71,72,9
CQUAD4,29,50,71,35,34,72
CQUAD4,34,50,9,72,73,10
CQUAD4,35,50,72,34,33,73
CQUAD4,36,50,10,73,74,11
CQUAD4,37,50,73,33,32,74
CQUAD4,38,50,11,74,75,12
CQUAD4,39,50,74,32,31,75
CQUAD4,40,50,12,75,76,13
CQUAD4,41,50,75,31,30,76
CQUAD4,42,50,13,76,77,14
CQUAD4,43,50,76,30,29,77
CTRIA3,44,50,14,79,15
CQUAD4,45,50,14,77,78,79
CQUAD4,46,50,77,29,28,78
CQUAD4,47,50,15,79,80,16
CQUAD4,48,50,79,78,81,80
CQUAD4,49,50,78,28,27,81
CQUAD4,50,50,16,80,83,17
CQUAD4,51,50,80,81,82,83
CQUAD4,52,50,81,27,26,82
CTRIA3,53,50,18,17,84
CQUAD4,54,50,17,83,85,84
CQUAD4,55,50,83,82,86,85
CQUAD4,56,50,82,26,25,86
CQUAD4,57,50,18,84,89,90
CQUAD4,58,50,84,85,86,89
CQUAD4,59,50,85,86,87,88
CQUAD4,60,50,86,25,97,87
CQUAD4,61,50,90,89,91,19
CQUAD4,62,50,89,88,92,91
CQUAD4,63,50,88,87,93,92
CQUAD4,64,50,87,37,24,93
CQUAD4,65,50,19,91,96,20
CQUAD4,66,50,91,92,95,96
CQUAD4,67,50,92,93,94,95
CQUAD4,68,50,93,24,21,94
CQUAD4,69,50,24,23,22,21
PSHELL,50,40,1.0,40
MAT1,40,1.7+7,,0.28
MATS1,40,,PLASTIC,0.0,1,1,4.5+4
SPC1,100,1,1,2,3,4,18,19,+S1
+S1,20,50,57,90
SPC1,100,2,1
SPC1,100,1,1,33,32,31
SPCD,10,33,1,-0.00075
SPCD,10,32,1,-0.00075
SPCD,10,31,1,-0.00075
SPCD,20,33,1,-0.0015
SPCD,20,32,1,-0.0015
SPCD,20,31,1,-0.0015
SPCD,30,33,1,-0.003
SPCD,30,32,1,-0.003
SPCD,30,31,1,-0.003
FORCE,10,33,,0.00,-1.0,0.0,0.0
FORCE,10,32,,0.00,-1.0,0.0,0.0
FORCE,10,31,,0.00,-1.0,0.0,0.0
FORCE,20,33,,0.00,-1.0,0.0,0.0
FORCE,20,32,,0.00,-1.0,0.0,0.0
FORCE,20,31,,0.00,-1.0,0.0,0.0
```

```
FORCE,30,33,,0.00,-1.0,0.0,0.0
FORCE,30,32,,0.00,-1.0,0.0,0.0
FORCE,30,31,,0.00,-1.0,0.0,0.0
GRID,300,,0.020,0.030,0.0,,123456
GRID,290,,0.02,0.040,0.0,,123456
GRID,280,,0.020,0.0425,0.0,,123456
GRID,270,,0.020,0.045,0.0,,123456
GRID,260,,0.020,0.0475,0.0,,123456
GRID,250,,0.020,0.050,0.0,,123456
GRID,970,,0.02,0.055,0.0,,123456
CGAP,300,43,30,300,,,,0
CGAP,290,53,29,290,,,,0
CGAP,280,63,28,280,,,,0
CGAP,270,73,27,270,,,,0
CGAP,260,83,26,260,,,,0
CGAP,250,93,25,250,,,,0
CGAP,970,103,97,970,,,,0
PGAP,43,0.0043,0.043,1.0+6,1.0+1,1.-8
PGAP,53,0.0053,0.053,1.0+6,1.0+1,1.-8
PGAP,63,0.0063,0.063,1.0+6,1.0+1,1.-8
PGAP,73,0.0073,0.073,1.0+6,1.0+1,1.-8
PGAP,83,0.0083,0.083,1.0+6,1.0+1,1.-8
PGAP,93,0.0093,0.093,1.0+6,1.0+1,1.-8
PGAP,103,0.0103,0.103,1.0+6,1.0+1,1.-8
NLPARM,10,5,,AUTOCON,,-40,W,YES,+P1
+P1,,,,2
NLPARM,20,20,,AUTOCON,,-40,W,YES,+P2
+P2,,,,2
NLPARM,30,5,,AUTOCON,,-40,W,YES,+P3
+P3,,,,2
ENDDATA
```